

Generalized Interpolating Discrete Diffusion

Dimitri von Rütte¹ Janis Fluri¹ Yuhui Ding¹ Antonio Orvieto^{2,3} Bernhard Schölkopf^{1,2,3} Thomas Hofmann¹

Abstract

While state-of-the-art language models achieve impressive results through next-token prediction, they have inherent limitations such as the inability to revise already generated tokens. This has prompted exploration of alternative approaches such as discrete diffusion. However, masked diffusion, which has emerged as a popular choice due to its simplicity and effectiveness, reintroduces this inability to revise words. To overcome this, we generalize masked diffusion and derive the theoretical backbone of a family of general interpolating discrete diffusion (GIDD) processes offering greater flexibility in the design of the noising processes. Leveraging a novel diffusion ELBO, we achieve compute-matched state-of-the-art performance in diffusion language modeling. Exploiting GIDD’s flexibility, we explore a hybrid approach combining masking and uniform noise, leading to improved sample quality and unlocking the ability for the model to correct its own mistakes, an area where autoregressive models notoriously have struggled. Our code and models are open-source: <https://github.com/dvruette/gidd/>

1. Introduction

Gleaning the structure of our world from observations is a fundamental mechanism of intelligence. While biological organisms do so routinely, the ability of machines to do the same has been limited until recently. Advances in deep learning have since unlocked this capability through training larger models with more capacity on ever-increasing amounts of data (Krizhevsky et al., 2012; Silver et al., 2017; Brown et al., 2020; OpenAI et al., 2023). Deep generative models have seen remarkable improvements stemming from both scaling training compute and algorithmic breakthroughs (Kumar et al., 2023). As the name suggests, generative models face the difficult task of generating new,

¹Data Analytics Lab, Department of Computer Science, ETH Zurich ²ELLIS Institute Tübingen, Tübingen AI Center ³Max Planck Institute for Intelligent Systems, Tübingen. Correspondence to: Dimitri von Rütte <dvruette@ethz.ch>.

Preprint. Copyright 2025 by the author(s).

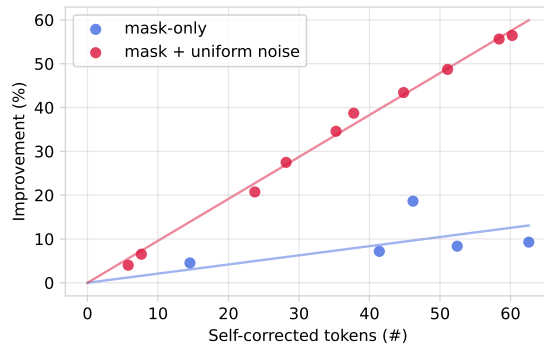


Figure 1. Training a diffusion model using GIDD on a combination of masking and uniform noise teaches it to identify and correct its own mistakes. By iteratively replacing bad tokens with better ones (as determined by the model), sample quality (as per generative PPL via Gemma 2 9B) improves by up to 55%.

realistic samples, where “realistic” usually refers to samples with high likelihood under some reference distribution.

For certain data distributions such as natural images or natural language, the information content of any given sample can be quite overwhelming. A common strategy to ease the burden on the generative model is to break up the task of generating a single sample into multiple inference steps, each being much simpler in isolation, but recovering the full distribution when recombined. The most prevalent example of this, especially for natural language, is autoregressive modeling (Bengio et al., 2000), where the task of generating a sentence (or sequence) is decomposed into generating one word (or token) at a time, with each new word serving as additional context for the next word. While extraordinarily successful on a wide range of data modalities (van den Oord et al., 2016a,b; Radford et al., 2018), there are some inherent challenges to this approach. First and most obviously, generating a sequence of length N necessarily requires N invocations of the model. This is not a problem if N is small but can become expensive as N grows to large numbers. Secondly, long-term dependencies and coherence can pose a challenge. If, at any point, a wrong token is sampled or a previous token becomes incompatible with newly sampled tokens, there is no way to correct it. Considerable effort has gone into solving this limitation, for example by post-training with reinforcement learning (RL) to teach sequential reasoning over multiple autoregressive steps (OpenAI et al., 2024; DeepSeek-AI et al., 2025).

Machine learning are is a field to study of research in artificial intelligence during which and the development [...]

Republic of DeltaWorld of Warcraft has made some significant improvements to game it in their the most recent improvement update, the “Death in the Vengeance” change “End of the World” update.

Mexico City is the largest city in France Mexico. With an estimated population of 22,752,000 22,000,000 [...]

Suppose Alice has 5 apples. If Alice gives 2 all of her the apples to Bob, she is left with zero apples.

Table 1. Examples of self-correction (green replaces red) by our GIDD+ BASE model trained with 20% uniform noise. The model is able to correct grammatical mistakes, improve word choices, and even improve factuality without being explicitly trained to do so.

Denoising diffusion models (Sohl-Dickstein et al., 2015) propose a different way of decomposing the generative task which can address both limitations. Instead of splitting the sample into elements of a sequence, we gradually decrease the information content of the entire sample by degrading it through the addition of some form of noise until, eventually, the information content reaches zero. The generative task then consists of reversing this degradation process, gradually adding information back in until the full sample is restored. This decouples the number of model invocations from the size of the sample since the number of steps we take to fill in the missing information can be chosen freely. For natural images, an obvious and suitable degradation is the progressive addition of per-pixel Gaussian noise. This choice yields a simple training objective that works well in practice and forms the basis of state-of-the-art image generation models (Ho et al., 2020; Kingma et al., 2023). The success of image diffusion models has spurred interest in applications to other domains and modalities, including discrete data like text (Austin et al., 2023). Unfortunately, Gaussian diffusion cannot be naively applied to discrete data as there is not necessarily a notion of distance or similarity, at least not one that is straightforward to measure. Instead, discrete diffusion models have converged on a degradation process consisting of gradually removing (“masking”) tokens until none are left (Austin et al., 2023; Shi et al., 2024; Sahoo et al., 2024). The task of the model then becomes to reconstruct the original sequence by “filling in the blanks” until all masked tokens have been filled in. This can also be thought of as autoregressive generation in a randomized order, and indeed reintroduces one of its inherent limitations: Once a token is filled in, it can no longer be changed, and any intermediate errors will necessarily propagate to the final sample.

This elicits the realization that the noising process is an integral part of a diffusion model with potentially fundamental implications on its strengths and limitations. Drawing motivation from this, our work aims to illuminate the design space of discrete diffusion models by exploring alternative diffusion processes. Our contributions are two-fold:

- On the theoretical side, in Section 3 we extend the framework of masked diffusion to general interpolating discrete diffusion (GIDD) processes. GIDD offers

great flexibility in the choice of noising process while still admitting closed-form solutions for the cumulative state transitions and the diffusion Evidence Lower Bound (ELBO).

- On the practical side, in Sections 4 and 5 we use our theoretical insights to facilitate practical improvements, achieving compute-matched state-of-the-art results thanks to an improved training objective (Sec. 5.2), as well as increasing sample quality and unlocking self-correction capabilities (Fig. 1, Tab. 1) thanks to the addition of uniform noise (Sec. 5.4).

2. Discrete Diffusion Models

As the name suggests, discrete diffusion models act on a discrete state space \mathcal{Z} . Given some initial state $X \in \mathcal{Z}$ sampled from the data distribution $q_0(X)$, the sample is gradually degraded through a Markov chain Z_1, \dots, Z_T with $Z_t \in \mathcal{Z}$, $Z_{t+1} \sim q_t(Z_{t+1}|Z_t)$, and $Z_1 = X$ until reaching some (easy-to-sample) prior distribution $p_T(Z_T)$. The denoising task then becomes to learn the backward kernel of this Markov chain, such that we can (approximately) reverse the degradation process for any Z_T sampled from the prior distribution. Oftentimes, the state space is structured as a sequence (of length L) of tokens from a vocabulary V , i.e. $Z_t = (z_t^{(1)}, \dots, z_t^{(L)})$ with $z_t^{(i)} \in V$. In this case, it is common to add noise to each token independently such that it suffices to look at the forward and backward noising trajectory of any token z_t in isolation. This is possible if the initial state X is known, which it is during training but not during inference. The model must therefore learn to make predictions without this knowledge, inferring as much as possible about X from its noisy version, the sequence Z_t .

2.1. Interpolating Masked Diffusion

Masked diffusion models (MDM) have seen widespread adoption by the community (Ou et al., 2024; Shi et al., 2024; Sahoo et al., 2024; Nie et al., 2024; Hu & Ommer, 2024) due to their simplicity and good performance. The core idea is to progressively replace tokens with a special [MASK] token until every token has been replaced. As such, the denoising task for the model to learn is to “fill in the blanks” given some context. This noising process results in a Markov chain with marginal transitions that can

be written as a linear interpolation between mask and data:

$$q_t(z_t|x) = \text{Cat}(z_t; \alpha_t \mathbf{x} + \beta_t \mathbf{m}), \quad (1)$$

where $\beta_t = 1 - \alpha_t$, \mathbf{x} and \mathbf{m} denote the one-hot encoding of the data x and the masking token m respectively,¹ and $0 \leq \alpha_t \leq 1$ determines the signal-to-noise ratio (SNR) at the current time t . The Evidence Lower Bound (ELBO) of MDM takes the form of a simple weighted reconstruction loss of the missing tokens. Specifically, with \mathbf{x}_θ denoting a neural network that predicts the distribution of x given a partially noised sequence $Z_t = (z_t^{(1)}, \dots, z_t^{(L)})$, the negative ELBO is given by

$$\begin{aligned} & -\log p(x) \\ & \leq \mathbb{E}_{t,z_t} \left[\frac{\alpha'_t}{1 - \alpha_t} \delta_{z_t, m} \mathbf{x}^\top \log \mathbf{x}_\theta(Z_t, t) \right] + C, \end{aligned} \quad (2)$$

where $t \sim \mathcal{U}(0, 1)$ and $z_t \sim q_t(z_t|x)$, with δ denoting the Kronecker delta function. Recall that the input to \mathbf{x}_θ is the entire noisy sequence Z_t whereas everything else happens for each token independently.

3. Generalized Interpolating Diffusion

Limitations of masked diffusion. Despite its popularity, masked diffusion has some fundamental limitations. Most obviously, due to the way the underlying Markov chain is defined, a token can never be changed again once it has been filled in, which is analogous to autoregressive prediction. This can lead to the accumulation of errors or some tokens becoming incompatible as more tokens are unmasked, and with no way to fix them, they inadvertently persist to the final result. Another, less severe limitation is the fact that only masked tokens carry a loss signal, as unmasked tokens are always completely noise-free. Like with BERT, this results in a smaller effective batch size which can lead to slower convergence compared to autoregressive models (Devlin et al., 2019; Clark et al., 2020).

Beyond masked diffusion. To resolve these limitations, we would like to expand our horizon to a more diverse set of diffusion processes. A natural solution like in BERT (Devlin et al., 2019) would be to use a combination of masking and uniform noise. This would address both limitations described above: Not only do we gain the ability to change already-unmasked tokens during sampling, but we also obtain a more informative training task, as every token in the sequence (whether masked or not) could potentially be corrupted and thus require correction. With the model learning to distinguish between “correct” and “incorrect” tokens, it may also learn to correct its own mistakes, a hope that will later be confirmed (Sec. 5.4).

¹Throughout, we will use bold letters to denote vectors, which, in reference to a token, denotes the one-hot encoding of the token.

However, there are some technical challenges to training a diffusion model on some specific, desirable diffusion trajectory. The canonical training objective—the diffusion ELBO—cannot be derived without knowledge of the Markovian state transitions, but crafting a Markov chain with specific emerging properties (e.g. “halfway in the diffusion process, 40% of tokens should be masked, 40% should be unperturbed, and 20% should be random”) is generally a non-trivial inverse problem. Instead of solving this inverse problem for a specific combination of masking and uniform noise, and to gain the necessary flexibility to design an effective model, we aim to generalize interpolating diffusion from mask-only to arbitrary (time-varying) interpolants. Specifically, we introduce the Generalized Interpolating Discrete Diffusion process (GIDD), a family of diffusion models with marginal forward transitions

$$q_t(z_t|x) = \text{Cat}(z_t; \alpha_t \mathbf{x} + \beta_t \boldsymbol{\pi}_t), \quad (3)$$

where $\boldsymbol{\pi}_t$ can be any probability distribution that changes smoothly over time. Notably, masked diffusion is a special case of GIDD for $\boldsymbol{\pi}_t = \mathbf{m}$. We will show the existence of a Markov chain that results in these marginals for any suitable α_t and $\boldsymbol{\pi}_t$ and derive its conditional transitions as well as the associated ELBO necessary for likelihood training.

3.1. Forward Process

GIDD is designed to allow maximal flexibility over the type of noise added to the data at any point in time. It consists of a mixing rate α_t , which defines the signal-to-noise ratio over time, and a mixing distribution $\boldsymbol{\pi}_t$, which defines what distribution the data is noised towards at any given time. We refer to the combination of these two functions as the “mixing schedule” of our diffusion process.

Definition 3.1 (Mixing Rate). Let the (cumulative) mixing rate α_t, β_t with $\beta_t = 1 - \alpha_t$ be a time-differentiable decreasing function $\alpha_t: [0, 1] \mapsto [0, 1]$ where the initial value $\alpha_0 = 1$ means no mixing and the final value $\alpha_1 = 0$ is complete mixing. This determines the SNR with $\text{SNR} = \alpha_t/\beta_t$.

Definition 3.2 (Mixing Distribution). Let the mixing distribution $\boldsymbol{\pi}_t$ be a time-dependent probability vector, i.e. a time-differentiable function $\boldsymbol{\pi}_t: [0, 1] \mapsto \Delta^{|V|-1}$ where $\Delta^{|V|-1}$ denotes the $|V|$ -dimensional simplex.² The distribution $\boldsymbol{\pi}_t$ determines the type of noise that is added to the data at any time t . As a consequence, $\boldsymbol{\pi}_1$ represents the prior distribution of our diffusion process.

Ultimately, we want to find a diffusion Markov chain with marginals as postulated in Equation (3), but to arrive at this conclusion we will have to work our way up from the underlying discrete-time Markov chain to the continuous-time state transitions, to the closed-form cumulative transitions.

²The d -dimensional simplex Δ^{d-1} is defined as the set of all points $x \in \mathbb{R}^d$ with $x_i \geq 0$ and $\sum_i x_i = 1$.

Proposition 3.3 (GIDD Conditional Transitions). *Let $\alpha_t, \beta_t = 1 - \alpha_t$ denote the mixing rate and let π_t denote the mixing distribution. Then there exists a continuous-time Markov chain with transition probabilities from state z_s to z_t at times $s < t$ given by*

$$q_{t|s}(z_t|z_s) = \text{Cat}(z_t; Q_{t|s} \mathbf{z}_s), \quad Q_{t|s} = \alpha_{t|s} I + \beta_{t|s} \pi_{t|s} \mathbf{1}^\top,$$

where $\alpha_{t|s} = \frac{\alpha_t}{\alpha_s}$, $\beta_{t|s} \pi_{t|s} = \beta_t \pi_t - \frac{\alpha_t}{\alpha_s} \beta_s \pi_s$, and $\mathbf{1}$ denotes the $|V|$ -dim. vector of all ones.

Proof. Let us discretize time into a Δ -spaced mesh for some arbitrary $\Delta > 0$, i.e. assume that we can write $t = \Delta i$ with $i \in \mathbb{Z}$ for any t . We then define the instantaneous mixing schedule³ $\dot{\alpha}_t$ and $\dot{\beta}_t \dot{\pi}_t$ as

$$\dot{\alpha}_{\Delta i} = \frac{\alpha_{\Delta(i+1)}}{\alpha_{\Delta i}},$$

$$\dot{\beta}_{\Delta i} \dot{\pi}_{\Delta i} = \beta_{\Delta(i+1)} \pi_{\Delta(i+1)} - \frac{\alpha_{\Delta(i+1)}}{\alpha_{\Delta i}} \beta_{\Delta i} \pi_{\Delta i}.$$

The instantaneous transition probability is now defined as

$$\dot{q}_t(z_{t+\Delta}|z_t) = \text{Cat}(z_{t+\Delta}; \dot{Q}_t \mathbf{z}_t), \quad \dot{Q}_t = \dot{\alpha}_t I + \dot{\beta}_t \dot{\pi}_t \mathbf{1}^\top.$$

The instantaneous transitions induce a discrete-time Markov chain with the desired mixing properties as defined by our mixing schedule. We now turn to our main objective: the cumulative transition matrix $Q_{t|s}$ of this Markov chain, which is defined as $Q_{t|s} = \prod_{i=s/\Delta}^{t/\Delta-1} \dot{Q}_{\Delta i}$. We need to show that $Q_{t|s} = \alpha_{t|s} I + \beta_{t|s} \pi_{t|s} \mathbf{1}^\top$. To this end, we are going to inductively unroll a single step to find recursive formulas for $\alpha_{t|s}$ and $\beta_{t|s} \pi_{t|s}$. First, note that the base case $t = s$ is simply $Q_{s|s} = I$ with $\alpha_{s|s} = 1$ and $\beta_{s|s} \pi_{s|s} = 0$ as we must remain in the same state. Next, assume that the induction hypothesis holds for $Q_{t|s}$. We then have

$$\begin{aligned} Q_{t+\Delta|s} &= \dot{Q}_t Q_{t|s} \\ &= [\dot{\alpha}_t I + \dot{\beta}_t \dot{\pi}_t \mathbf{1}^\top] \cdot [\alpha_{t|s} I + \beta_{t|s} \pi_{t|s} \mathbf{1}^\top] \\ &= \dot{\alpha}_t \alpha_{t|s} I + \dot{\beta}_t (\alpha_{t|s} \dot{\pi}_t \mathbf{1}^\top I + \beta_{t|s} \dot{\pi}_t (\mathbf{1}^\top \pi_{t|s}) \mathbf{1}^\top) \\ &\quad + \dot{\alpha}_t \beta_{t|s} \pi_{t|s} \mathbf{1}^\top \\ &= \dot{\alpha}_t \alpha_{t|s} I + \dot{\beta}_t (\alpha_{t|s} + \beta_{t|s}) \dot{\pi}_t \mathbf{1}^\top + \dot{\alpha}_t \beta_{t|s} \pi_{t|s} \mathbf{1}^\top \\ &= \underbrace{\dot{\alpha}_t \alpha_{t|s}}_{-\alpha_{t+\Delta|s}} I + \underbrace{(\dot{\beta}_t \dot{\pi}_t + \dot{\alpha}_t \beta_{t|s} \pi_{t|s})}_{\beta_{t+\Delta|s} \pi_{t+\Delta|s}} \mathbf{1}^\top, \end{aligned}$$

where we use the fact that $\mathbf{1}^\top \pi_{t|s} = 1$ and $\alpha_{t|s} + \beta_{t|s} = 1$ (as per Lemma H.1, App. H.1). Having found recursive formulas for $\alpha_{t|s}$ and $\beta_{t|s} \pi_{t|s}$ we can now apply telescoping to find the desired closed-form solutions (see App. H.2 for details), proving the original claim for any $\Delta > 0$. In particular, the proof also holds in the limit of $\Delta \rightarrow 0$ as long as the

³Note that while we use the dot-notation ($\dot{\alpha}$) to signify instantaneous changes, this is not to be confused with the time-derivative, which we denote by a prime (α').

limits $\lim_{\Delta \rightarrow 0} \dot{\alpha}_{\Delta i}$ and $\lim_{\Delta \rightarrow 0} \dot{\beta}_{\Delta i} \dot{\pi}_{\Delta i}$ exist. Differentiability of α_t and π_t , as required by Definitions 3.1 and 3.2, is sufficient for this to be the case. \square

Corollary 3.4. *The cumulative transition probabilities of the Markov chain from Proposition 3.3 are given by*

$$q_t(z_t|x) = \text{Cat}(z_t; Q_t \mathbf{x}), \quad Q_t = \alpha_t I + \beta_t \pi_t \mathbf{1}^\top.$$

Proof. The claim follows directly from Proposition 3.3 with $Q_t = Q_{t|0}$ and using the fact that $\alpha_0 = 1, \beta_0 = 0$. \square

With this, we have successfully constructed a Markov chain with the desired marginals outlined in Equation (3). For deriving the ELBO later on, we also need the transition rates of the corresponding Continuous-Time Markov Chain (CTMC), which is defined as follows.

Definition 3.5 (CTMC Forward Transition). *For some start time s and end time $t = s + \Delta$ with $\Delta \rightarrow 0$, we have*

$$q_{t|s}(z_t|z_s) = \delta_{z_s, z_t} + R_t(z_s, z_t) \Delta + o(\Delta),$$

where R_t is called the forward transition rate. Little- o notation is used for denoting asymptotically sub-linear terms.

We now characterize the CTMC forward rate of GIDD.

Lemma 3.6 (GIDD Forward Rate). *The CTMC forward rate matrix R_t of GIDD is given by*

$$R_t(z_s, z_t) = \frac{\alpha'_t}{\alpha_t} \delta_{z_s, z_t} + \mathbf{z}_t^\top \left((\beta_t \pi_t)' - \frac{\alpha'_t}{\alpha_t} \beta_t \pi_t \right),$$

where α'_t and $(\beta_t \pi_t)'$ denote the time-derivative of the respective mixing function.

Proof. By performing a first-order Taylor expansion on $q_{t|s}(z_t|z_s)$ and rearranging the result, we arrive at the desired expression. See Appendix H.3 for details. \square

3.2. Backward Process

We choose the same parameterization of the backward process as prior work (Sohl-Dickstein et al., 2015; Austin et al., 2023). The canonical model distribution for diffusion $p_\theta(z_s|z_t)$ is given by

$$p_\theta(z_s|z_t) = q_{t|s}(z_t|z_s) \frac{q_s(z_s|\mathbf{x}_\theta)}{q_t(z_t|\mathbf{x}_\theta)}, \quad (4)$$

with shorthand notation $q_t(z_t|\mathbf{x}_\theta) := \text{Cat}(z_t; Q_t \mathbf{x}_\theta(Z_t, t))$, where $\mathbf{x}_\theta(Z_t, t)$ is a neural network that predicts the distribution of x given the noised sequence Z_t . The ELBO derivation also requires the CTMC backward rate $\hat{R}_t(z_t, z_s)$, but refer to Appendix H.4 for details.

3.3. ELBO

In order to train a GIDD model, we need a differentiable way to estimate its likelihood. The Evidence Lower Bound (ELBO) serves this purpose: By maximizing a lower bound, we implicitly also maximize the (worst-case) likelihood of our model. For the ELBO, we need the forward and backward rate of GIDD, which we have already derived. Then, starting with a slightly modified version of the ELBO from Campbell et al. (2022), we plug in our forward and backward rates $R_t(z_s, z_t)$ and $\hat{R}_t(z_t, z_s)$ and simplify to obtain Theorem 3.7 (complete proof in App. H.5).

Theorem 3.7 (GIDD ELBO). *Let α_t , β_t and π_t be a mixing schedule as defined in Definitions 3.1, and 3.2 with marginal forward distribution $q_t(z_t|x)$ as defined in Equation 3. Let further $w_t(z_t, x)$ be a weighting function defined as*

$$w_t(z_t, x) = \frac{1}{q_t(z_t|x)} \mathbf{z}_t^\top \left((\beta_t \pi_t)' - \frac{\alpha_t'}{\alpha_t} \beta_t \pi_t \right).$$

Then, the continuous-time negative ELBO (CT-NELBO) of the corresponding diffusion model is given by

$$\begin{aligned} -\log p(x) \leq \\ \mathbb{E}_{t, z_t} [w_t(z_t, x) (D_{KL}(q_t(z_s|x) \| q_t(z_s|\mathbf{x}_\theta)) + r_\theta(z_t, x))] \\ + \mathbb{E}_t [\alpha_t'/\alpha_t] + C, \end{aligned}$$

where $r_\theta(z_t, x) = \frac{q_t(z_t|x)}{q_t(z_t|\mathbf{x}_\theta)} - \log \frac{q_t(z_t|x)}{q_t(z_t|\mathbf{x}_\theta)}$, $t \sim \mathcal{U}(0, 1)$, and $z_t \sim q_t(\cdot|x)$, and with C denoting the ELBO constant

$$C = \mathbb{E}_{q_0(z_0|x)} [\log p(x|z_0)] - D_{KL}(q_1(z_1|x) \| p_1(x_1)).$$

Since GIDD is a strictly more general form of the widely used masked diffusion paradigm (Ou et al., 2024; Shi et al., 2024; Sahoo et al., 2024), we expect the canonical MDM ELBO to emerge from the GIDD ELBO by choosing an appropriate mixing schedule, which is indeed what we find by setting $\pi_t = \mathbf{m}$ (proof in Appendix I).

Corollary 3.8 (Equivalence to MDM). *If $\pi_t = \mathbf{m}$, then, for any valid noise schedule α_t , the GIDD ELBO reduces to the MDM ELBO (Eq. 2).*

Interpretation. Taking a closer look at the GIDD ELBO, we notice that it consists of solving two tasks jointly:

- 1) The first task is to match the model to the marginal forward distribution of some sample x given its noised version z_t at the current noise level by minimizing the KL-divergence between the two distributions. Notably, this term is minimized if and only if the two distribution are the same.
- 2) The second task is to minimize $r_\theta(z_t, x)$. While this term doesn't have a direct intuitive interpretation, the task consists of matching the marginal probability of z_t and is minimized at 1 if and only if $q_t(z_t|x) = q_t(z_t|\mathbf{x}_\theta)$. Interest-

ingly, both tasks have the same global optimum, which has direct implications on the global minimum of the ELBO.

Proposition 3.9. *For any mixing schedule α_t , β_t and π_t , the GIDD CT-NELBO has a global minimum of zero (up to the ELBO constant C), which is reached if and only if $q_t(z_t|x)$ and $q_t(z_t|\mathbf{x}_\theta)$ are the same for all x , t , and z_t .*

Proof (sketch). By plugging the joint global minimum of $D_{KL}(q_t(z_s|x) \| q_t(z_s|\mathbf{x}_\theta)) = 0$ and $r_\theta(z_t, x) = 1$ into the GIDD ELBO, we can simplify the resulting expression to $\mathbb{E}_t [\beta_t \mathbf{1}^\top \pi_t'] + C$. Using the fact that π_t is a probability vector, i.e. $\mathbf{1}^\top \pi_t = 1$, we deduce that $\mathbf{1}^\top \pi_t' = 0$, canceling out the remaining term. See Appendix H.6 for details. \square

This is good news, since it tells us that the mixing schedule theoretically does not limit the best-possible model. In conclusion, the GIDD ELBO is a straight-forward and flexible training objective that can be applied out-of-the-box to any interpolating diffusion model.

3.4. Sampling

Given some sampling schedule $0 \approx t_0 < t_1 < \dots < t_T \approx 1$ and some neural network \mathbf{x}_θ , we employ ancestral sampling by discretizing time along the chosen mesh. Specifically, starting with a sequence of all mask tokens, i.e. $z_{t_T} = m$ for all z_{t_T} , we iteratively sample $p_\theta(z_{t_{i-1}}|z_{t_i})$ for $i = T, \dots, 1$:

$$z_{t_{i-1}} \sim q_{t_i|t_{i-1}}(z_{t_i}|z_{t_{i-1}}) \frac{q_{t_{i-1}}(z_{t_{i-1}}|\mathbf{x}_\theta(Z_{t_i}, t_i))}{q_{t_i}(z_{t_i}|\mathbf{x}_\theta(Z_{t_i}, t_i))} \quad (5)$$

Self-Correction Step. In addition, we propose a fixed-point iteration to improve generated samples by resampling some tokens according to the model's judgement. More precisely, we give the fully denoised sample Z_{t_0} to the model and sample the resulting distribution with some temperature τ . Then, of all sampled tokens different from Z_{t_0} , we select the one with the highest model likelihood and commit it. This is repeated until convergence (details in App. C).

4. Mixing Schedule

While GIDD can be used for masked diffusion, our original motivation for introducing a generalized framework was to explore the combination of masking and uniform noise. To this end, we design a mixing schedule that keeps the masked prior distribution but allows for configurable amounts of uniform noise in between. We use p_u to denote the amount of uniform noise: For the sake of interpretability, the expected fraction of uniform tokens should reach a maximum of p_u at the midpoint between data and noise ($t = 1/2$). With these desiderata in mind, we define our mixing rate and mixing distribution (Def. 3.1 and 3.2):

$$\alpha_t = \frac{1-t}{C_t}, \quad \beta_t \pi_t = \frac{t}{C_t} \mathbf{m} + \frac{c_t}{C_t} \mathbf{1}, \quad (6)$$

where $c_t = B t^{\frac{\gamma}{2}} (1-t)^{\frac{\gamma}{2}}$, $C_t = 1 + N c_t$, N denotes the vocabulary size, and B is a constant chosen such that

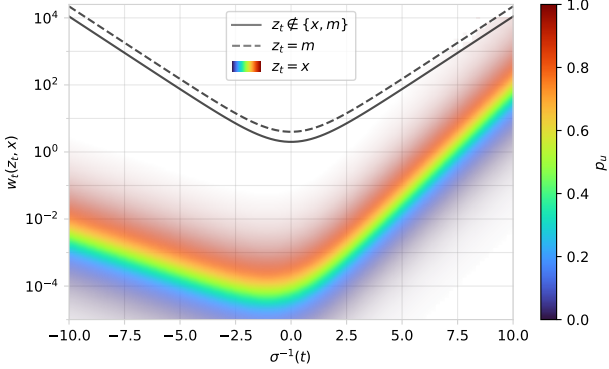


Figure 2. ELBO weights grow exponentially for very low/high noise levels, causing poor optimization if not handled carefully. While masked and uniform token weights are almost constant, noise-free token weights vary heavily depending on p_u .

the desired uniform token ratio is reached. The marginal forward distribution then becomes

$$q_t(z_t|x) = \frac{1}{C_t}((1-t)\mathbf{x} + t\mathbf{m} + c_t\mathbf{1}). \quad (7)$$

To reach the uniform noise level p_u at $t = 1/2$, we need to set $B = \frac{2^\gamma p_u}{N(1-p_u)}$ (proof in App. H.7). The GIDD ELBO involves some additional constants and factors, which requires deriving the corresponding time-derivatives (see App. H.8 for details). Note that setting $p_u = 0.0$ again recovers masked diffusion. Finally, we set $\gamma = 1$, but there are many possible choices for hyperparameters introduced in this section.

4.1. Training Objective

Before starting our experiments, we need to solve one last issue, which will yield great performance gains. Taking a closer look at the ELBO weights $w_t(z_t, x)$, we find that their behaviour for $t \rightarrow 0$ and $t \rightarrow 1$ is quite extreme. Consider the three possible cases $z_t = x$, $z_t = m$, and $z_t \notin \{x, m\}$. Plotting the weights $w_t(z_t, x)$ over time⁴ reveals that the weight grows exponentially for very low/high noise levels in all three cases (Figure 2). This can be problematic since these low/high noise samples provide little to no training signal as the model’s job of denoising becomes either trivial or impossible, yet can easily drown out all other samples in the batch. To counteract this issue, we propose two weighting schemes that reduce the influence of extreme samples, hence emphasizing intermediate noise levels where the training task is informative.

The simple and obvious solution is to clamp the weights to some maximal value w_{\max} , so we define

$$\tilde{w}_t^{\text{clamp}}(z_t, x) = \min(w_{\max}, w_t(z_t, x)). \quad (8)$$

Through preliminary experiments, we find $w_{\max} = 1$ to be best, so this is used throughout. Note that clamping

⁴ $\sigma^{-1}(t)$ denotes the inverse sigmoid function and can be thought of as the log-SNR when ignoring the effect of C_t .

Model (SMALL)	Train. toks.	PPL (↓)
<i>Autoregressive</i>		
GPT2 (Radford et al., 2019)	unk.	23.40
Llama 110M (retrain.)	262B	16.11
<i>Diffusion</i>		
MD4* (Shi et al., 2024)	524B	21.80
MDLM* (Sahoo et al., 2024)	262B	23.21
MDM (reimpl.)	262B	23.36
GIDD+ (ours; $p_u = 0.0$)	262B	22.29

Table 2. Our best GIDD model outperforms the compute-matched MDM (reimpl.) baseline, which in turn closely matches results from the MDM literature in terms of validation PPL on OWT.

*Numbers reported by the original paper.

Model (SMALL)	PPL (↓)		
	$p_u = 0.0$	$p_u = 0.1$	$p_u = 0.2$
MDM (reimpl.)	24.37	-	-
GIDD (ours)	24.36	26.88	28.22
+ weight clipping	23.23	25.09	26.40
+ dynamic weights	23.24	23.90	24.64
+ weight decay	23.05	23.67	24.38

Table 3. PPL of GIDD ($p_u = 0.0$) and MDM match closely, as expected from their theoretical equivalence. Significant gains come from choosing the right weighting function, especially in the $p_u > 0$ regime. The final best setting includes dynamic loss weights \tilde{w}_t^{dyn} and weight decay and is also referred to as *GIDD+*.

mostly affects the weights of mask and uniform tokens. A more principled approach may aim to keep the maximum loss weight constant while preserving the relative weights between masked, uniform, and noise-free tokens. We call this the dynamic weighting function and define it as

$$\tilde{w}_t^{\text{dyn}}(z_t, x) = w_{\max}(1 + \delta_{z_t, m} + (Be^{-\frac{\lambda_t}{2}} - 1)\delta_{z_t, x}), \quad (9)$$

where $\lambda_t = \log \frac{\alpha_t}{1-\alpha_t}$ is the log-SNR. The relative weights ($2 / 1 / Be^{-\frac{\lambda_t}{2}}$) are determined empirically. Note that re-weighting the ELBO like this is equivalent to sampling t from a non-uniform distribution (Kingma & Gao, 2023).

5. Experiments

5.1. Experimental Setup

While discrete diffusion models are a natural fit for any discrete data, we focus our attention specifically on language modeling as it is one of the most prevalent tasks in modern machine learning. To this end, we adopt the OpenWebText (OWT) dataset (Gokaslan et al., 2019) since there exists a rich literature for both autoregressive and diffusion models trained on this dataset. We follow prior work (Sahoo et al., 2024; Shi et al., 2024) in terms of architecture and scale and use the DiT architecture (Peebles & Xie, 2023) with the GPT2 tokenizer (Radford et al., 2019) and train SMALL

Generalized Interpolating Discrete Diffusion

Size	Model	Train. toks.	ARC-e	ARC-c	BoolQ	Hellaswag	PIQA	OBQA	WinoG.	Avg.
SMALL	GPT2	unk.	43.81	19.03	48.72	28.92	62.89	16.40	51.62	38.77
	Llama (retrain.)	262B	40.53	25.51	46.21	33.14	62.73	28.40	50.75	41.04
	MDM (reimpl.)	262B	30.98	23.63	50.52	31.11	54.13	<u>28.00</u>	49.41	38.25
	GIDD+ ($p_u = 0.0$)	262B	30.98	23.55	50.43	<u>31.87</u>	<u>56.42</u>	26.60	51.70	38.79
	GIDD+ ($p_u = 0.0$)	131B	<u>31.57</u>	<u>24.57</u>	50.92	31.36	56.31	27.80	52.57	39.30
BASE	GIDD+ ($p_u = 0.0$)	131B	32.58	24.40	50.86	36.62	58.05	29.2	51.54	40.46
1.1B	TinyLlama*	500B	55.47	32.68	55.99	61.47	73.56	36.80	59.43	53.63
	MDM*	500B	48.74		62.17	51.83	69.53	33.40		

Table 4. Our best GIDD+ model in terms of zero-shot benchmark accuracy outperforms MDM (reimpl.) and even surpasses GPT2-small, although it still lags behind our Llama-based autoregressive baseline. Best scores among SMALL models and diffusion models are bolded and underlined respectively. *Numbers reported by [Zhang et al. \(2024\)](#) for TinyLlama and by [Nie et al. \(2024\)](#) for MDM 1.1B.

(110M) and BASE (320M) models on 131B or 262B tokens, depending on the experiment (training details in App. E).

5.2. Ablation Study

The goal of our ablation study is to answer three main questions: 1) Does GIDD with our mixing schedule and $p_u = 0.0$ recover MDM as theory predicts? 2) How does the addition of uniform noise affect performance? And 3) what is the benefit of the weighting functions from Sec. 4.1?

To this end, we train SMALL GIDD models on OWT with varying levels of uniform noise $p_u \in \{0.0, 0.1, 0.2\}$. We also train our reimplementation of MDM on the same setup. The final validation perplexity (PPL) of these runs is reported in Table 3. Regarding the first question, we find that the training trajectories as well as the final performance of MDM and GIDD ($p_u = 0.0$) match almost perfectly with a respective validation PPL of 24.37 and 24.36. Our MDM reimplementation also closely matches the compute-matched MDLM ([Sahoo et al., 2024](#)) baseline (Table 2) considering the slight differences in hyperparameters.

However, adding uniform noise to the diffusion process, we find that perplexity degrades slightly as the problem becomes more difficult, yet benefiting expressivity as we will see later (Sec. 5.4). This difference likely stems from an increase in task complexity: The combination of masking and uniform noise requires solving multiple tasks jointly, and therefore needs more model capacity. This is supported by the observation that all noise levels scale consistently with model size, with the highest noise setting even showing some signs of improved scaling behavior (see App. A).

Our custom weighting schemes bring non-trivial performance gains to both the mask-only and hybrid noise settings, and particularly the dynamic weighting scheme \tilde{w}_t^{dyn} closes the gap significantly. We hypothesize that the difference between $\tilde{w}_t^{\text{clamp}}$ and \tilde{w}_t^{dyn} is due to the importance of noise-free tokens, which have zero weight if $p_u = 0.0$ but cannot be ignored otherwise. Therefore, keeping the true relative weights between different token types seems to be

beneficial if $p_u > 0$. Finally, a moderate amount of weight decay (0.02) improves both training and validation loss, as suggested by [D’Angelo et al. \(2024\)](#). The best configuration uses dynamic loss weights \tilde{w}_t^{dyn} and 0.02 weight decay, which we refer to as GIDD+ from hereon out.

5.3. Downstream Performance

We evaluate our models’ language understanding capabilities on a range of benchmarks. Based on the increased difficulty of the hybrid noise setting, we do not expect $p_u > 0$ models to outperform the mask-only case, which is indeed what we find (App. B). Instead, we focus on comparing the best SMALL GIDD+ model to MDM and autoregressive baselines, namely GPT2 ([Radford et al., 2019](#)) and a retrained Llama ([Touvron et al., 2023a](#)). For reference, we also include two 1.1B parameter models, one autoregressive ([Zhang et al., 2024](#)) and one masked diffusion ([Nie et al., 2024](#)). Our benchmark suite consists of ARC-e and ARC-c ([Clark et al., 2018](#)), BoolQ ([Clark et al., 2019](#)), Hellaswag ([Zellers et al., 2019](#)), PIQA ([Bisk et al., 2019](#)), OpenBookQA ([Mihaylov et al., 2018](#)), and WinoGrande ([Sakaguchi et al., 2019](#)). We find that average accuracy generally correlates well with validation PPL (Tab. 4). Among diffusion models, the best performing model is GIDD+ ($p_u = 0.0$) trained for only 131B tokens, surpassing models trained for twice as long. This is likely due to overfitting on spurious patterns in the training data, which still decreases validation loss but does not translate to downstream performance. Notably, the best diffusion model, GIDD+, outperforms the autoregressive GPT2, though the difference in training data makes a fair comparison somewhat difficult. Indeed, the best autoregressive model, Llama (retrain.), still comes out on top overall, although the margin is less than one percentage point on average. For GIDD models trained with uniform noise, the trend is in line with validation PPL, with more uniform noise generally hurting accuracy (see App. B). Nevertheless, performance improves consistently with increased model size, and tentative signs suggest that the gap may shrink with increased scale (App. A).

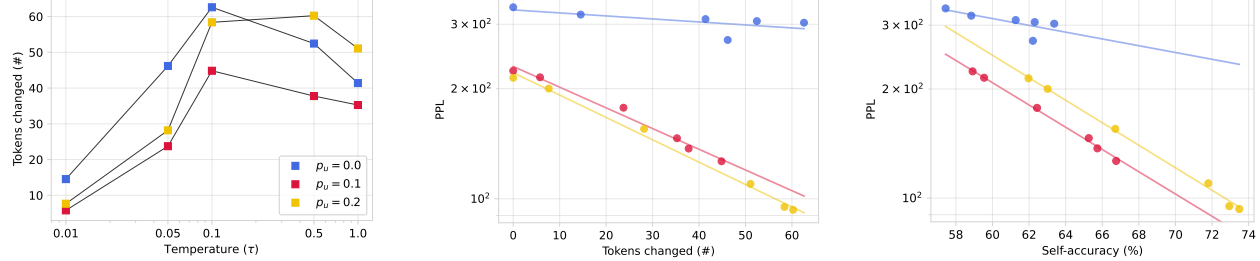


Figure 3. From left to right: (a) Self-correction using GIDD+ (BASE) models resamples up to 10% of tokens independent of the uniform noise level. A temperature of $\tau \in [0.1, 0.5]$ is found to be most effective. (b) For models trained on uniform noise, the more changes, the better. The mask-only model, though, is unable to improve quality despite resampling as many tokens. (c) Looking at the correlation between self-accuracy and generative PPL reveals that hybrid models are significantly better at judging the quality of their own samples.

5.4. Self-Correction

So far, we have seen a pattern of models trained with uniform noise being outperformed by their mask-only counterpart, but we have yet to consider the main motivation for its addition: By teaching the model to distinguish between “correct” and “incorrect” tokens, we hope to unlock the ability for the model to correct its own mistakes via the proposed self-correction step (Sec. 3.4). In order to quantify sample quality, we use “generative perplexity”, a metric that computes the likelihood of generated samples under a more capable model (in our case Gemma 2 9B, [Gemma Team \(2024\)](#)), where a high likelihood is considered to be a sign of high quality. While this metric has many flaws (see App. G), it is common in the literature ([Lou et al., 2024](#); [Sahoo et al., 2024](#)). We find that, though absolute numbers are difficult to interpret in isolation, it is still useful for comparing models in relative terms. In addition to generative PPL, we also measure the self-accuracy of the model, i.e. what percentage of tokens the model “is happy with” in the sense that it assigns maximal likelihood to any token in the sequence.

For BASE models, both metrics improve consistently with more self-correction steps, resulting in higher self-accuracy and lower generative PPL (Fig. 3). Qualitative evaluation also confirms this (see examples in Tab. 1, 6). For the mask-only model, while the self-correction step still resamples the same number of tokens, this does not translate to improved gen. PPL or self-accuracy, showing that the ability to self-correct is only acquired if some amount of uniform noise is present during training. Despite this, the mask-only model does appear to improve slightly, which is likely due to numerical limitations: For numerical stability, we actually set p_u to a very small value instead of 0.0, empirically resulting in approx. 10 (out of 262'144) random tokens per batch. Indeed, the MDM (reimpl.) baseline does not exhibit any self-correction abilities at all and in fact makes samples worse during the self-correction step (App. C).

Notably, the sample quality of models trained on uniform noise is already better before self-correction, with especially significant improvements over mask-only models for low

inference-compute settings with a generative PPL of 387 for GIDD+ (SMALL; $p_u = 0.1$) at 32 steps compared to 904 for $p_u = 0.0$ and 1302 for MDM (App. D). So, training on uniform noise seems to stabilize the generation process when the model gets its own outputs as input, resulting in better sample quality in terms of gen. PPL despite having a slightly worse validation PPL. This suggests that some amount of self-correction may already be happening during the denoising process, prompting the question of whether improvements during self-correction can be explained simply by the increased iteration count. However, while more denoising steps monotonically improve sample quality, this plateaus at a PPL of around 200 for BASE models (App. D). Using self-correction, though, we can go below a PPL of 100, showing additional, non-trivial improvements.

6. Related Work

Our work builds on a line of discrete diffusion research, with [Austin et al. \(2023\)](#) first introducing the diffusion ELBO to discrete Markov chains, [Campbell et al. \(2022\)](#) extending it to continuous time, [Lou et al. \(2024\)](#) deriving an alternative ELBO based on concrete score matching, and concurrent work by [Shi et al. \(2024\)](#), [Sahoo et al. \(2024\)](#) and [Ou et al. \(2024\)](#) proposes a simplified objective for masked diffusion. The discrete diffusion process has also been a subject of study, with [Gu et al. \(2022\)](#) using a combination of masking and uniform noise for vector-quantized image generation, but providing no empirically study the effect of combining the two types of noise. [He et al. \(2022\)](#) propose a noise schedule that degrades different tokens at different rates, depending on their “difficulty” as estimated using BERT. Continuous diffusion has also been adapted to discrete data by doing Gaussian diffusion in some embedding space ([Li et al., 2022](#); [Gulrajani & Hashimoto, 2023](#)).

Diffusion-like approaches have also been applied to discrete data, with discrete flow matching ([Gat et al., 2024](#)) extending the flow-matching paradigm ([Liu et al., 2022](#); [Lipman et al., 2022](#)) and Bayesian flow networks ([Graves et al., 2024](#)) adopting the perspective of denoising directly

in probability space rather than collapsing the distribution after each step.

Finally, the idea of denoising a combination of masking and uniform noise was popularized by BERT (Devlin et al., 2019), where it was proposed in the context of representation learning, and has been applied to discrete diffusion for vector-quantized image generation (Gu et al., 2022).

7. Conclusion

We have introduced a new family of generalized interpolating diffusion processes (dubbed GIDD) and successfully applied it in practice. While the extreme scale required to train overall state-of-the-art language models is out of scope for this work, we see great potential in the methods and results described here, but also in diffusion language models more broadly: Self-correction is an area that next-token prediction notoriously has struggled with, but as we discovered, this capability comes naturally to diffusion models given the right type of noise. Our work also presents a step towards closing the gap in pure language modeling performance between diffusion and autoregressive models, achieving state-of-the-art perplexity for compute-matched diffusion models thanks to a re-weighted version of our newly proposed GIDD ELBO. Beyond our work, discrete diffusion models respond well to scaling training-time compute like their next-token prediction counterpart, but also provide a natural way to scale test-time compute. By choosing the number of denoising steps, and now also by choosing the number of self-correction iterations, one can trade off speed and accuracy depending on the setting. All in all, and given that GIDD opens a design space yet to be explored fully, this may render diffusion language models a promising competitor to autoregressive models in the future.

Impact Statement

This paper presents work whose goal is to advance the technical state-of-the-art in an area of Machine Learning. It shares potential societal consequences with much of the work in the general area of language modeling and foundation models.

Acknowledgment

Antonio Orvieto and Bernhard Schölkopf acknowledge the financial support of the Hector Foundation.

References

Austin, J., Johnson, D. D., Ho, J., Tarlow, D., and van den Berg, R. Structured denoising diffusion models in discrete state-spaces, 2023. URL <https://arxiv.org/abs/2107.03006>.

Bengio, Y., Ducharme, R., and Vincent, P. A neural probabilistic language model. *Advances in neural information processing systems*, 13, 2000.

Bisk, Y., Zellers, R., Bras, R. L., Gao, J., and Choi, Y. PIQA: Reasoning about physical commonsense in natural language, 2019. URL <https://arxiv.org/abs/1911.11641>.

Brown, T. B., Mann, B., Ryder, N., Subbiah, M., Kaplan, J., Dhariwal, P., Neelakantan, A., Shyam, P., Sastry, G., Askell, A., Agarwal, S., Herbert-Voss, A., Krueger, G., Henighan, T., Child, R., Ramesh, A., Ziegler, D. M., Wu, J., Winter, C., Hesse, C., Chen, M., Sigler, E., Litwin, M., Gray, S., Chess, B., Clark, J., Berner, C., McCandlish, S., Radford, A., Sutskever, I., and Amodei, D. Language models are few-shot learners, 2020. URL <https://arxiv.org/abs/2005.14165>.

Campbell, A., Benton, J., Bortoli, V. D., Rainforth, T., Deligiannidis, G., and Doucet, A. A continuous time framework for discrete denoising models, 2022. URL <https://arxiv.org/abs/2205.14987>.

Clark, C., Lee, K., Chang, M.-W., Kwiatkowski, T., Collins, M., and Toutanova, K. BoolQ: Exploring the surprising difficulty of natural yes/no questions, 2019. URL <https://arxiv.org/abs/1905.10044>.

Clark, K., Luong, M.-T., Le, Q. V., and Manning, C. D. ELECTRA: Pre-training text encoders as discriminators rather than generators, 2020. URL <https://arxiv.org/abs/2003.10555>.

Clark, P., Cowhey, I., Etzioni, O., Khot, T., Sabharwal, A., Schoenick, C., and Tafjord, O. Think you have solved question answering? Try ARC, the AI2 reasoning challenge, 2018. URL <https://arxiv.org/abs/1803.05457>.

D’Angelo, F., Andriushchenko, M., Varre, A., and Flammarion, N. Why do we need weight decay in modern deep learning?, 2024. URL <https://arxiv.org/abs/2310.04415>.

DeepSeek-AI et al. DeepSeek-V3 technical report, 2024. URL <https://arxiv.org/abs/2412.19437>.

DeepSeek-AI et al. DeepSeek-R1: Incentivizing reasoning capability in llms via reinforcement learning, 2025. URL <https://arxiv.org/abs/2501.12948>.

Devlin, J., Chang, M.-W., Lee, K., and Toutanova, K. BERT: Pre-training of deep bidirectional transformers for language understanding, 2019. URL <https://arxiv.org/abs/1810.04805>.

Gao, L., Tow, J., Abbasi, B., Biderman, S., Black, S., DiPofi, A., Foster, C., Golding, L., Hsu, J., Le Noac'h, A., Li, H., McDonell, K., Muennighoff, N., Ociepa, C., Phang, J., Reynolds, L., Schoelkopf, H., Skowron, A., Sutawika, L., Tang, E., Thite, A., Wang, B., Wang, K., and Zou, A. A framework for few-shot language model evaluation, 07 2024. URL <https://zenodo.org/records/12608602>.

Gat, I., Remez, T., Shaul, N., Kreuk, F., Chen, R. T. Q., Synnaeve, G., Adi, Y., and Lipman, Y. Discrete flow matching, 2024. URL <https://arxiv.org/abs/2407.15595>.

Gemma Team. Gemma. 2024. doi: 10.34740/KAGGLE/M/3301. URL <https://www.kaggle.com/m/3301>.

Gokaslan, A., Cohen, V., Pavlick, E., and Tellex, S. Open-WebText corpus. <http://Skylion007.github.io/OpenWebTextCorpus>, 2019.

Grattafiori, A. et al. The Llama 3 herd of models, 2024. URL <https://arxiv.org/abs/2407.21783>.

Graves, A., Srivastava, R. K., Atkinson, T., and Gomez, F. Bayesian flow networks, 2024. URL <https://arxiv.org/abs/2308.07037>.

Gu, S., Chen, D., Bao, J., Wen, F., Zhang, B., Chen, D., Yuan, L., and Guo, B. Vector quantized diffusion model for text-to-image synthesis, 2022. URL <https://arxiv.org/abs/2111.14822>.

Gulrajani, I. and Hashimoto, T. B. Likelihood-based diffusion language models, 2023. URL <https://arxiv.org/abs/2305.18619>.

Gumbel, E. J. *Statistical theory of extreme values and some practical applications: a series of lectures*, volume 33. US Government Printing Office, 1954.

He, Z., Sun, T., Wang, K., Huang, X., and Qiu, X. DiffusionBERT: Improving generative masked language models with diffusion models, 2022. URL <https://arxiv.org/abs/2211.15029>.

Ho, J., Jain, A., and Abbeel, P. Denoising diffusion probabilistic models, 2020. URL <https://arxiv.org/abs/2006.11239>.

Hoffmann, J., Borgeaud, S., Mensch, A., Buchatskaya, E., Cai, T., Rutherford, E., de Las Casas, D., Hendricks, L. A., Welbl, J., Clark, A., Hennigan, T., Noland, E., Millican, K., van den Driessche, G., Damoc, B., Guy, A., Osindero, S., Simonyan, K., Elsen, E., Rae, J. W., Vinyals, O., and Sifre, L. Training compute-optimal large language models, 2022. URL <https://arxiv.org/abs/2203.15556>.

Hu, V. T. and Ommer, B. [MASK] is all you need, 2024. URL <https://arxiv.org/abs/2412.06787>.

Kingma, D. P. and Ba, J. Adam: A method for stochastic optimization, 2017. URL <https://arxiv.org/abs/1412.6980>.

Kingma, D. P. and Gao, R. Understanding diffusion objectives as the elbo with simple data augmentation, 2023. URL <https://arxiv.org/abs/2303.00848>.

Kingma, D. P., Salimans, T., Poole, B., and Ho, J. Variational diffusion models, 2023. URL <https://arxiv.org/abs/2107.00630>.

Krizhevsky, A., Sutskever, I., and Hinton, G. E. ImageNet classification with deep convolutional neural networks. In Pereira, F., Burges, C., Bottou, L., and Weinberger, K. (eds.), *Advances in Neural Information Processing Systems*, volume 25. Curran Associates, Inc., 2012. URL https://proceedings.neurips.cc/paper_files/paper/2012/file/c399862d3b9d6b76c8436e924a68c45b-Paper.pdf.

Kumar, S., Musharaf, D., Musharaf, S., and Sagar, A. K. A comprehensive review of the latest advancements in large generative ai models. In *International Conference on Advanced Communication and Intelligent Systems*, pp. 90–103. Springer, 2023.

Li, X. L., Thickstun, J., Gulrajani, I., Liang, P., and Hashimoto, T. B. Diffusion-LM improves controllable text generation, 2022. URL <https://arxiv.org/abs/2205.14217>.

Lipman, Y., Chen, R. T. Q., Ben-Hamu, H., Nickel, M., and Le, M. Flow matching for generative modeling, 2022. URL <https://arxiv.org/abs/2210.02747>.

Liu, X., Gong, C., and Liu, Q. Flow straight and fast: Learning to generate and transfer data with rectified flow, 2022. URL <https://arxiv.org/abs/2209.03003>.

Lou, A., Meng, C., and Ermon, S. Discrete diffusion modeling by estimating the ratios of the data distribution, 2024. URL <https://arxiv.org/abs/2310.16834>.

Mihaylov, T., Clark, P., Khot, T., and Sabharwal, A. Can a suit of armor conduct electricity? A new dataset for open book question answering, 2018. URL <https://arxiv.org/abs/1809.02789>.

Nguyen, M., Baker, A., Neo, C., Roush, A., Kirsch, A., and Shwartz-Ziv, R. Turning up the heat: Min-p sampling for creative and coherent llm outputs, 2024. URL <https://arxiv.org/abs/2407.01082>.

Nie, S., Zhu, F., Du, C., Pang, T., Liu, Q., Zeng, G., Lin, M., and Li, C. Scaling up masked diffusion models on text, 2024. URL <https://arxiv.org/abs/2410.18514>.

OpenAI et al. GPT-4 technical report. 2023. URL <https://arxiv.org/abs/2303.08774>.

OpenAI et al. OpenAI o1 system card, 2024. URL <https://arxiv.org/abs/2412.16720>.

Ou, J., Nie, S., Xue, K., Zhu, F., Sun, J., Li, Z., and Li, C. Your absorbing discrete diffusion secretly models the conditional distributions of clean data, 2024. URL <https://arxiv.org/abs/2406.03736>.

Peebles, W. and Xie, S. Scalable diffusion models with transformers, 2023. URL <https://arxiv.org/abs/2212.09748>.

Radford, A., Narasimhan, K., Salimans, T., and Sutskever, I. Improving language understanding by generative pre-training. 2018. URL https://cdn.openai.com/research-covers/language-unsupervised/language-understanding_paper.pdf.

Radford, A., Wu, J., Child, R., Luan, D., Amodei, D., and Sutskever, I. Language models are unsupervised multitask learners. 2019.

Sahoo, S. S., Arriola, M., Schiff, Y., Gokaslan, A., Marroquin, E., Chiu, J. T., Rush, A., and Kuleshov, V. Simple and effective masked diffusion language models, 2024. URL <https://arxiv.org/abs/2406.07524>.

Sakaguchi, K., Bras, R. L., Bhagavatula, C., and Choi, Y. WinoGrande: An adversarial Winograd schema challenge at scale, 2019. URL <https://arxiv.org/abs/1907.10641>.

Shi, J., Han, K., Wang, Z., Doucet, A., and Titsias, M. K. Simplified and generalized masked diffusion for discrete data, 2024. URL <https://arxiv.org/abs/2406.04329>.

Silver, D., Schrittwieser, J., Simonyan, K., Antonoglou, I., Huang, A., Guez, A., Hubert, T., Baker, L., Lai, M., Bolton, A., et al. Mastering the game of go without human knowledge. *nature*, 550(7676):354–359, 2017.

Sohl-Dickstein, J., Weiss, E. A., Maheswaranathan, N., and Ganguli, S. Deep unsupervised learning using nonequilibrium thermodynamics, 2015. URL <https://arxiv.org/abs/1503.03585>.

Tange, O. Gnu Parallel 20241222 ('Bashar'), December 2024. URL <https://doi.org/10.5281/> zenodo.14550073. GNU Parallel is a general parallelizer to run multiple serial command line programs in parallel without changing them.

Touvron, H., Lavril, T., Izacard, G., Martinet, X., Lachaux, M.-A., Lacroix, T., Rozière, B., Goyal, N., Hambro, E., Azhar, F., Rodriguez, A., Joulin, A., Grave, E., and Lample, G. LLaMA: Open and efficient foundation language models, 2023a. URL <https://arxiv.org/abs/2302.13971>.

Touvron, H., Martin, L., Stone, K., et al. Llama 2: Open foundation and fine-tuned chat models, 2023b. URL <https://arxiv.org/abs/2307.09288>.

van den Oord, A., Dieleman, S., Zen, H., Simonyan, K., Vinyals, O., Graves, A., Kalchbrenner, N., Senior, A., and Kavukcuoglu, K. WaveNet: A generative model for raw audio, 2016a. URL <https://arxiv.org/abs/1609.03499>.

van den Oord, A., Kalchbrenner, N., Vinyals, O., Espeholt, L., Graves, A., and Kavukcuoglu, K. Conditional image generation with PixelCNN decoders, 2016b. URL <https://arxiv.org/abs/1606.05328>.

Wei, J., Tay, Y., Bommasani, R., Raffel, C., Zoph, B., Borgeaud, S., Yogatama, D., Bosma, M., Zhou, D., Metzler, D., Chi, E. H., Hashimoto, T., Vinyals, O., Liang, P., Dean, J., and Fedus, W. Emergent abilities of large language models, 2022. URL <https://arxiv.org/abs/2206.07682>.

Zellers, R., Holtzman, A., Bisk, Y., Farhadi, A., and Choi, Y. HellaSwag: Can a machine really finish your sentence?, 2019. URL <https://arxiv.org/abs/1905.07830>.

Zhang, P., Zeng, G., Wang, T., and Lu, W. TinyLlama: An open-source small language model, 2024. URL <https://arxiv.org/abs/2401.02385>.

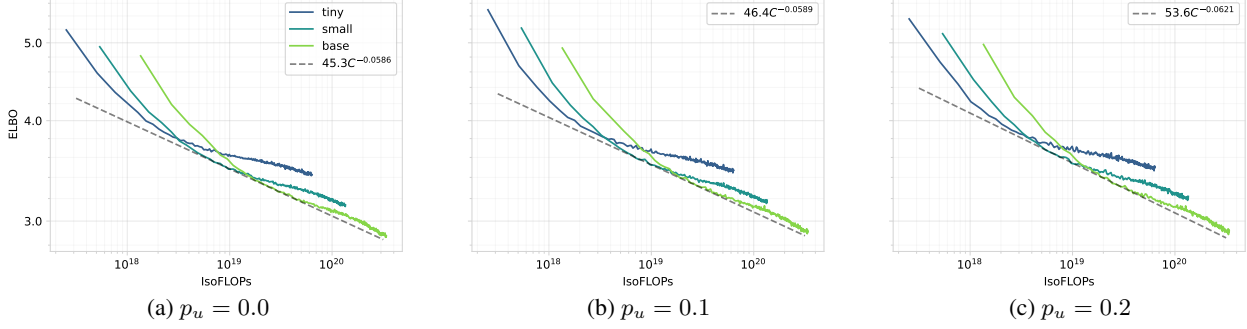


Figure 4. Plotting the compute-efficient frontier reveals different scaling behaviors for different uniform noise levels, revealing that training with uniform noise benefits slightly more from scaling compute compared to the mask-only setting.

A. Uniform Noise and Model Capacity

In Section 5, we have observed that the addition of uniform noise can pose a challenge, and even with improvements to the weighting function, the likelihood of trained models decreases as the proportion of uniform noise increases. Intuitively speaking, this is not entirely surprising since the addition of uniform noise makes the training task strictly more difficult: No longer can the model take for granted that every unmasked token is correct. Instead, it has to consider every token in the context and, if necessary, replace it with the correct one. This intuitive explanation suggests that the reason for the observed discrepancy in performance may be a lack of model capacity, in which case we would expect larger models to be less affected by the addition of uniform noise.

To test this hypothesis, we scale the number of parameters while keeping the training horizon constant and train models of sizes TINY, SMALL, and BASE on different uniform noise levels $p_u \in \{0.0, 0.1, 0.2\}$. We then plot the compute-efficient frontier as an exponential fit to the pareto-optimal validation ELBO (Figure 4). For computing IsoFLOPs of our models, we follow the method from Hoffmann et al. (2022), App. F. Due to resource constraints, our setup is somewhat limited: The sample size is limited to three different compute budgets for each noise level, the largest of which is still comparatively small at 3.3×10^{20} FLOPs. As a point of reference, many signature capabilities of modern LLMs only start emerging around 10^{22} FLOPs (Wei et al., 2022), which is still 2 orders of magnitude higher than our largest compute budget. With this being said, we do indeed observe a consistent albeit small trend of higher levels of uniform noise scaling better with more compute. While the mask-only setting ($p_u = 0.0$) has a scaling exponent of -0.0586 , adding uniform noise increases the scaling exponent to -0.0589 and -0.0621 for $p_u = 0.1$ and $p_u = 0.2$ respectively. Extrapolating this trend predicts that the $p_u = 0.2$ setting will overtake $p_u = 0.0$ around 10^{21} FLOPs, a compute budget that is routinely reached by mid-to large-scale training runs (Brown et al., 2020; Touvron et al., 2023b; Grattafiori et al., 2024; DeepSeek-AI et al., 2024). However, it has to be stressed that the limitations of our setup make such a prediction highly unreliable. For example, the optimal amount of uniform noise may change with model size and/or compute budget, or certain hyperparameters like the learning rate may have different optimal values depending on p_u . Nevertheless, the observed scaling behavior is promising and warrants further investigation.

B. GIDD Downstream Performance

Benchmark accuracies for GIDD+ models of all three sizes (TINY, SMALL, BASE) and all uniform noise levels ($p_u \in \{0.0, 0.1, 0.2\}$) are given in Table 5. We find that performance improves consistently with model size, regardless of uniform noise level. However, the models trained with uniform noise slightly but consistently lag behind the mask-only model.

C. Self-Correction Step

Self-Correction Algorithm. Our self-correction algorithm is a fixed-point iteration that can be applied to any generated sample that is fully (or partially) denoised. The high-level idea is to query the model to identify tokens that it thinks are wrong and should be replaced, and to then iteratively replace a single token at a time so as to avoid reintroducing conflicting tokens. A pseudocode implementation is given in Algorithm 1. In practice, we find that convergence often comes in the form of oscillation between two or more equally-good states (in terms of self-accuracy), so we additionally implement early-stopping based on self-accuracy. An early-stopping patience of 32 is found to work well.

Generalized Interpolating Discrete Diffusion

Size	Model	Train. toks.	ARC-e	ARC-c	BoolQ	Hellaswag	PIQA	OBQA	WinoG.	Avg.
TINY	GIDD+ ($p_u = 0.0$)	131B	28.28	24.49	49.97	27.78	54.62	26.20	51.30	37.52
	GIDD+ ($p_u = 0.1$)	131B	27.69	23.21	50.89	26.75	55.28	24.60	52.25	37.24
	GIDD+ ($p_u = 0.2$)	131B	26.73	23.12	50.18	25.61	51.52	27.40	49.33	36.27
SMALL	GIDD+ ($p_u = 0.0$)	131B	31.57	24.57	50.92	31.36	56.31	27.80	52.57	39.30
	GIDD+ ($p_u = 0.1$)	131B	28.45	21.93	50.73	28.37	55.82	29.20	52.17	38.10
	GIDD+ ($p_u = 0.2$)	131B	27.99	22.87	50.46	26.92	52.94	26.40	50.04	36.80
BASE	GIDD+ ($p_u = 0.0$)	131B	32.58	24.40	50.86	36.62	58.05	29.2	51.54	40.46
	GIDD+ ($p_u = 0.1$)	131B	30.13	23.04	51.10	31.91	56.15	27.6	52.33	38.89
	GIDD+ ($p_u = 0.2$)	131B	28.75	24.15	50.95	29.82	53.81	26.8	49.25	37.65

Table 5. Downstream performance of GIDD increases consistently with model size, but hybrid noise models lag behind their mask-only counterparts across scales.

Algorithm 1 Self-Correction Step

Let $Z_t = (z_t^{(1)}, \dots, z_t^{(L)})$ be a (partially) denoised sequence up to noise level t .

Let $f_\theta(Z_t, t)$ denote a (trained) discrete denoising neural network.

while not converged **do**

$\mathbf{x}_\theta^{(1:L)} \leftarrow \text{softmax}(f_\theta(Z_t, t)/\tau)$

for $i \in \{1, \dots, L\}$ **do**

$z_t'^{(i)} \sim \text{Cat}(\mathbf{x}_\theta^{(i)})$

end for

$S \leftarrow \{i | i \in \{1, \dots, L\} \text{ and } z_t'^{(i)} \neq z_t^{(i)}\}$

$j \leftarrow \arg \max_{i \in S} \mathbf{x}_\theta^{(i)}(z_t'^{(i)})$

$z_t^{(j)} \leftarrow z_t'^{(j)}$

end while

Additional Results. In addition to the results for our BASE models given in the main text, we also report improvements for SMALL models, which are very comparable. A notable difference is that for SMALL models, $p_u = 0.1$ has a consistently lower generative PPL, suggesting that $p_u = 0.2$ is too much uniform noise for this size. We also include our MDM baseline, as the comparison between same-sized models is fair. Despite our GIDD+ ($p_u = 0.0$) exhibiting a weak but present ability to self-correct, MDM has no such ability and applying the self-correction step only makes the samples worse (Figure 5). The most likely cause for this difference are implementation details, where, for numerical stability, p_u is not actually set to zero, but to a very small value, which still results in approx. 10 (out of 262'144) random tokens per batch due to limited numerical precision. Alternative explanations may look at differences in hyperparameters, or the numerically non-zero weights on unmasked tokens in the GIDD setup. More examples from the self-correction experiment are given in Table 6.

D. Number of Denoising Steps

Comparing sample quality for different numbers of denoising steps, we find that, as one would expect, sample quality in terms of generative PPL improves consistently with more denoising steps, up to around 128-256 steps when a plateau is reached (Figure 6). Notably, the sample quality of models trained with uniform noise is significantly better compared to those trained without. This trend is especially strong for small numbers of denoising steps, suggesting that the self-correction capabilities may help in those scenarios.

E. Training Details

All our models are based on the DiT architecture (Peebles & Xie, 2023) and use the GPT2 tokenizer (Radford et al., 2019). We train models of three different sizes: TINY ($L = 6, H = 8, d = 512$; 28.4M non-emb. params.), SMALL ($L = 12, H = 12, d = 768$; 92.1M non-emb. params.), and BASE ($L = 24, H = 16, d = 1024$; 321.2M non-emb. params.), where L

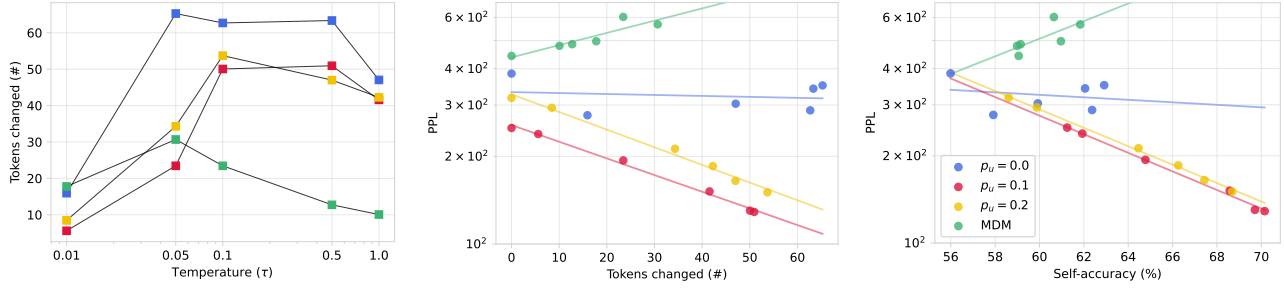


Figure 5. Self-correction results for our SMALL models. While the overall trend is the same as for BASE models, the best-performing model uses $p_u = 0.1$ instead of $p_u = 0.2$, suggesting that the ideal uniform noise ratio depends on model size. The MDM baseline is noticeably worse than the mask-only GIDD implementation, with self-correction yielding negative improvements, which is likely due to numerical limitations in the GIDD implementation.

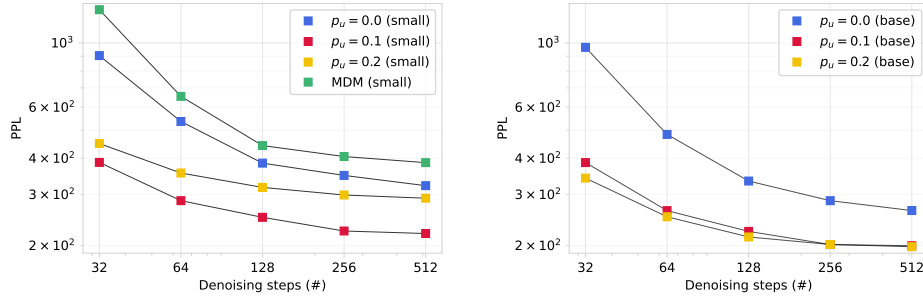


Figure 6. Generative PPL (via Gemma 2 9B) decreases monotonically with increasing numbers of denoising steps. Interestingly, the presence of uniform noise during training seems to benefit sample quality overall, but especially so for the low-step regime.

denotes the number of layers, H the number of attention heads, and d the dimensionality of hidden states. All models are trained with a context size of 512 tokens and batch size of 512 for 500k steps (resulting in a total of 131B training tokens) on a single node of 8 NVIDIA A100/H100-80GB GPUs in `bfloat16` precision using Pytorch’s mixed precision training (`torch.cuda.autocast`). For the sake of comparison with the literature, some models are trained for twice as long, resulting in 262B training tokens.

For optimization, we use the Adam optimizer (Kingma & Ba, 2017) with $\beta = (0.9, 0.99)$, $\epsilon = 10^{-9}$, and a learning rate of $5 \cdot 10^{-4}$. The learning rate is warmed up linearly for the first 10k steps and then decayed using a cosine schedule to 10% of the initial learning rate. We use weight decay 0.0 for our ablations (unless stated otherwise) and 0.02 for the final configuration, also referred to as GIDD+. We also use gradient clipping to a norm of 1.0.

For our noise schedule, we sample $t \sim \mathcal{U}(\epsilon, 1 - \epsilon)$ with $\epsilon = 10^{-4}$ using low-discrepancy sampling (Kingma et al., 2023). By default, all loss weights (including the unclamped ELBO weighting function) are clipped to 10^4 to prevent training instability. For sequences longer than 512 tokens we select a random window of 512 tokens, while short sequences are padded to a length of 512. Padding tokens are included in the loss calculation but are ignored in the ELBO.

F. Evaluation Details

For computing validation metrics, we reserve the last 100k samples ($\approx 1.25\%$) of the training set (OpenWebText). Validation samples that are longer than the context length are cropped to a random window for consistency with training.

For downstream performance evaluation, we use the `lm-eval-harness`⁵ (Gao et al., 2024) with a custom model that uses the ELBO to estimate per-token log-likelihoods. We only consider likelihood-based multiple-choice tasks where the per-token likelihood is computed over both the context and the completion (but not the padding), as preliminary experiments have found that this produces slightly better results. We use $T = 128$ evenly spaced samples (in $[\epsilon, 1 - \epsilon]$) for t to estimate the ELBO. Samples longer than the context size of our model (only applies to BoolQ) are truncated by taking the final N

⁵<https://github.com/EleutherAI/lm-evaluation-harness>

<i>Example 1</i>	
Republic of Deltaos have made some significant improvements to the patch in game.2: – “Death in the Vengeance” patch. Notable changes also included:	Republic of Deltaos have made some significant changes to the patch in game v2: The “Death in the Vengeance” patch. Notable changes are included:
Proflah Ring can be reached with the ring head up.	Profession Ring can be reached with the ring head up.
You can select characters from their application in choice.	You can select characters from their class of choice.
Growth returns below your output level when floating between the default dragon and the highest active rev tier.	Growth returns to your output level when floating between the default level and the highest level revamp.
Borg followed by Radiant World to earn and the coveted tutorial is now also available for Edition 12.	Borg followed by Radiant World to earn and the coveted tutorial is now also available at level 12.
<i>Example 2</i>	
a new industrial renaissance movement which uses the winner's would of GE technologies	a new industrial manufacturing platform which uses the lion's share of GE technologies
strong link between both US at manufacturing and integral US manufacturing production platform in America	strong link between the US industrial manufacturing and the US industrial manufacturing platform in Europe
<i>Example 3</i>	
short of the feeds public front music ming	instead of the free music fronting service
unlimited free music streaming and high-quality content, available whenever you Webs for your subscription.	unlimited free music streaming and high-quality content, available when you pay for a subscription.
<i>Example 4</i>	
Journal publishing has opened the world to these kinds scientists and scientists deserve an encouraging place to look.	Journal publishing has opened the world to these kinds, and scientists have an encouraging way to look.
Some researchers can discuss several papers, others are putting many many specific types of material.	Some researchers openly discuss their papers, others are putting many many specific types of papers.
Globality postulates the circumstances – researchers learn from the very reputation of other study team.	Globality postulates the circumstances – researchers learn from the good work of other research team.

Table 6. Examples from our self-correction experiments reveal a noticeable qualitative improvement: The model is able to correct grammatical mistakes (Ex. 2,3), improve coherence (Ex. 3), and improve the choice of words given the context (Ex. 1,4). The examples are from GIDD+ BASE ($p_u = 0.2$) with self-correction temperature $\tau = 0.1$.

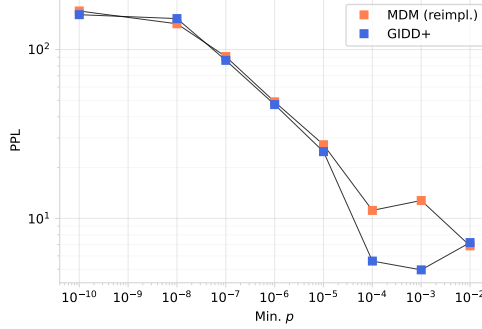


Figure 7. Generative perplexity as measured by GPT2-large decreases consistently as the min- p cutoff is increased. Unfortunately, this trend does not correlate with subjective quality, showing a major limitation of generative PPL with GPT2-large.

tokens, similar to context scrolling for autoregressive models.

Our generative perplexity is based on the `google/gemma-2-9b`⁶ model (Gemma Team, 2024) as it provides a good tradeoff between language modeling accuracy and efficiency. Prior work often relies on the GPT2-large model for generative PPL computation, but we believe that in order to draw meaningful conclusions, it is crucial to use a grading model that is sufficiently more capable than the graded model in order reasonably provide a proxy of the “ground truth” distribution of natural language.

We use the GNU parallel software (Tange, 2024) for streamlining the execution of our evaluation scripts.

G. Evaluating Generative Perplexity of Diffusion Models

Generative perplexity is an evaluation metric intended to measure the quality of generated samples using a grading model that is assumed to be approximately equal to the ground truth data distribution. Under this assumption, we deem samples with a high likelihood under the grading model to be higher quality, or at least more likely under the data distribution. While there are many potential issues with this approach, results can be particularly misleading if the grading model is a bad proxy for the true likelihood of samples. While prior work often relies on GPT2-large as a grading model, we find that this model suffers from failure modes that are typical for small (by today’s standards) models.

Before going into detail about the exact failure modes we observe, we need to discuss another peculiarity that arises when sampling from discrete diffusion models. A common approach to efficiently sample a categorical distribution is the Gumbel-max trick (Gumbel, 1954), which is used by Shi et al. (2024) (via JAX categorical sampling) and Sahoo et al. (2024). As noted by Shi et al. (2024) in App. G, this approach is somewhat numerically unstable and leads to an implicit regularization of the sampled distribution, effectively masking out very small probabilities (the authors report smaller than 10^{-8}). This is effectively a min- p sampling adapter, which has been found to improve sample quality of autoregressive language models alike (Nguyen et al., 2024). To study the effect of this min- p regularization, we explicitly implement it with a more numerically stable sampling algorithm based on binary search. Measuring the generative PPL as per GPT2-large for different values of p , we find a consistent decrease with the observed gen. PPL of ~ 90 around $p = 10^{-7}$ being consistent with what is reported for SMALL models in the literature (Figure 7).

However, as the cutoff probability increases, generative PPL drops to suspiciously low values. Indeed, manual inspection of the samples reveals that the sample quality deteriorates drastically for larger cutoffs (examples in Table 7). These samples exhibit low diversity and a lot of repetition, failure modes that are typical for small (autoregressive) language models. Despite this, these samples are deemed exceptionally likely by GPT2-large and hence are considered “high quality” under the generative PPL metric. This shows the importance of using more capable grading models that are able to pick up on these failure modes and the effect that sampling parameters can have on the outcome of these experiments. It also highlights the limitations of comparing absolute generative PPL numbers, as they can be misleading in isolation. While Gemma 2 9B also suffers from the failure mode described here to some extent, it should provide a much better proxy of the “true distribution” of natural language compared to the much weaker GPT2-large.

⁶<https://huggingface.co/google/gemma-2-9b>

Table 7. Samples generated with different min- p cutoff values. Despite generative PPL consistently decreasing for larger cutoffs, the sample quality starts to deteriorate drastically for values larger than $p \geq 10^{-4}$.

H. Proofs

H.1. Conditional Mixing Schedule

Lemma H.1. *If $\alpha_{t|s}$ and $\beta_{t|s}\boldsymbol{\pi}_{t|s}$ are defined as in Proposition 3.3, and if $\beta_{t|s} = \beta_t - \frac{\alpha_t}{\alpha_s}\beta_s$, then $\alpha_{t|s} + \beta_{t|s} = 1$ and $\boldsymbol{\pi}_{t|s}$ is a prob. vector, i.e. $\boldsymbol{\pi}_{t|s} > 0$ and $\mathbf{1}^\top \boldsymbol{\pi}_{t|s} = 1$.*

Proof. We have

$$\alpha_{t|s} + \beta_{t|s} = \frac{\alpha_t}{\alpha_s} + \beta_t - \frac{\alpha_t}{\alpha_s}\beta_s = \frac{\alpha_t}{\alpha_s}(1 - \beta_s) + \beta_t = \frac{\alpha_t}{\alpha_s}\alpha_s + \beta_t = \alpha_t + \beta_t = 1$$

and, using the fact that $\mathbf{1}^\top \boldsymbol{\pi}_t = 1, \forall t$ by Definition 3.2,

$$\mathbf{1}^\top \boldsymbol{\pi}_{t|s} = \mathbf{1}^\top \frac{1}{\beta_{t|s}}(\beta_{t|s}\boldsymbol{\pi}_{t|s}) = \frac{1}{\beta_{t|s}}\left(\beta_t \mathbf{1}^\top \boldsymbol{\pi}_t - \frac{\alpha_t}{\alpha_s}\beta_s \mathbf{1}^\top \boldsymbol{\pi}_s\right) = \frac{1}{\beta_{t|s}}\left(\beta_t - \frac{\alpha_t}{\alpha_s}\beta_s\right) = 1,$$

thus proving the claim. \square

H.2. GIDD Conditional Transitions

Proof of Telescoping in Prop. 3.3. Recall the recursive formulas for $\alpha_{t|s}$ and $\beta_{t|s}\boldsymbol{\pi}_{t|s}$:

$$\begin{aligned} \alpha_{t+\Delta|s} &= \dot{\alpha}_t \alpha_{t|s} \\ \beta_{t+\Delta|s}\boldsymbol{\pi}_{t|s} &= \dot{\beta}_t \dot{\boldsymbol{\pi}}_t + \dot{\alpha}_t \beta_{t|s}\boldsymbol{\pi}_{t|s} \end{aligned}$$

By unrolling the recursion and plugging in the definition of $\dot{\alpha}_t$ we then have

$$\alpha_{t|s} = \dot{\alpha}_{t-\Delta} \dot{\alpha}_{t-2\Delta} \cdots \dot{\alpha}_s \underbrace{\alpha_{s|s}}_{=1} = \prod_{i=s/\Delta}^{t/\Delta-1} \dot{\alpha}_{\Delta i} = \prod_{i=s/\Delta}^{t/\Delta-1} \frac{\alpha_{\Delta(i+1)}}{\alpha_{\Delta i}} = \frac{\alpha_{\Delta(t/\Delta)}}{\alpha_{\Delta(s/\Delta)}} = \frac{\alpha_t}{\alpha_s}.$$

Analogously, for $\beta_{t|s}\boldsymbol{\pi}_{t|s}$ we get

$$\begin{aligned} \beta_{t|s}\boldsymbol{\pi}_{t|s} &= \\ \dot{\beta}_{t-\Delta}\boldsymbol{\pi}_{t-\Delta} + \dot{\alpha}_{t-\Delta}\dot{\beta}_{t-2\Delta}\boldsymbol{\pi}_{t-2\Delta} + \cdots + \dot{\alpha}_{t-\Delta} \cdots \dot{\alpha}_{s+\Delta} \dot{\beta}_s \boldsymbol{\pi}_s + \dot{\alpha}_{t-\Delta} \cdots \dot{\alpha}_s \underbrace{\beta_{s|s}\boldsymbol{\pi}_{s|s}}_{=0} &= \sum_{i=s/\Delta}^{t/\Delta-1} \alpha_{t|\Delta(i+1)} \dot{\beta}_{\Delta i} \boldsymbol{\pi}_{\Delta i} \\ &= \sum_{i=s/\Delta}^{t/\Delta-1} \frac{\alpha_t}{\alpha_{\Delta(i+1)}} \left(\beta_{\Delta(i+1)} \boldsymbol{\pi}_{\Delta(i+1)} - \frac{\alpha_{\Delta(i+1)}}{\alpha_{\Delta i}} \beta_{\Delta i} \boldsymbol{\pi}_{\Delta i} \right) \\ &= \sum_{i=s/\Delta}^{t/\Delta-1} \left(\frac{\alpha_t}{\alpha_{\Delta(i+1)}} \beta_{\Delta(i+1)} \boldsymbol{\pi}_{\Delta(i+1)} - \frac{\alpha_t}{\alpha_{\Delta i}} \beta_{\Delta i} \boldsymbol{\pi}_{\Delta i} \right) \\ &= \frac{\alpha_t}{\alpha_t} \beta_t \boldsymbol{\pi}_t - \frac{\alpha_t}{\alpha_s} \beta_s \boldsymbol{\pi}_s = \beta_t \boldsymbol{\pi}_t - \frac{\alpha_t}{\alpha_s} \beta_s \boldsymbol{\pi}_s, \end{aligned}$$

yielding the desired expressions for $\alpha_{t|s}$ and $\beta_{t|s}\boldsymbol{\pi}_{t|s}$ and concluding the proof. \square

H.3. GIDD Forward Rate

Proof of Lemma 3.6. We need to show that the CTMC forward rate matrix R_t of GIDD is given by

$$R_t(z_s, z_t) = \frac{\alpha'_t}{\alpha_t} \delta_{z_s, z_t} + \mathbf{z}_t^\top \left((\beta_t \boldsymbol{\pi}_t)' - \frac{\alpha'_t}{\alpha_t} \beta_t \boldsymbol{\pi}_t \right),$$

where α'_t and $(\beta_t \boldsymbol{\pi}_t)'$ denote the time-derivative of the respective mixing function.

The proof follows the idea of Proof 2 in [Campbell et al. \(2022\)](#), App. B.2 to perform a first-order Taylor expansion on $q_{t|s}(z_t|z_s)$. To this end, let s be given and let $t = s + \Delta$ for some positive $\Delta \rightarrow 0$. Then, by Proposition 3.3 we have

$$q_{s+\Delta|s}(z_t|z_s) = \mathbf{z}_t^\top Q_{s+\Delta|s} \mathbf{z}_s = \mathbf{z}_t^\top (\alpha_{s+\Delta|s} \mathbf{z}_s + \beta_{s+\Delta|s} \boldsymbol{\pi}_{s+\Delta|s}).$$

We now linearize $\alpha_{s+\Delta|s}$ and $\beta_{s+\Delta|s} \boldsymbol{\pi}_{s+\Delta|s}$ around s , resulting in

$$\begin{aligned}\alpha_{s+\Delta|s} &= \frac{\alpha_{s+\Delta}}{\alpha_s} = \frac{\alpha_s + \alpha'_s \Delta + o(\Delta)}{\alpha_s} = 1 + \frac{\alpha'_s}{\alpha_s} \Delta + o(\Delta), \\ \beta_{s+\Delta|s} \boldsymbol{\pi}_{s+\Delta|s} &= \beta_{s+\Delta} \boldsymbol{\pi}_{s+\Delta} - \frac{\alpha_{s+\Delta}}{\alpha_s} \beta_s \boldsymbol{\pi}_s \\ &= (\beta_s \boldsymbol{\pi}_s + (\beta_s \boldsymbol{\pi}_s)' \Delta + o(\Delta)) - \left(1 + \frac{\alpha'_s}{\alpha_s} \Delta + o(\Delta)\right) \beta_s \boldsymbol{\pi}_s \\ &= \left((\beta_s \boldsymbol{\pi}_s)' - \frac{\alpha'_s}{\alpha_s} \beta_s \boldsymbol{\pi}_s\right) \Delta + o(\Delta).\end{aligned}$$

Plugging these terms into $q_{s+\Delta}(z_t|z_s)$ yields

$$\begin{aligned}q_{s+\Delta|s}(z_t|z_s) &= \mathbf{z}_t^\top \left(\left(1 + \frac{\alpha'_s}{\alpha_s} \Delta + o(\Delta)\right) \mathbf{z}_s + \left((\beta_s \boldsymbol{\pi}_s)' - \frac{\alpha'_s}{\alpha_s} \beta_s \boldsymbol{\pi}_s\right) \Delta + o(\Delta) \right) \\ &= \delta_{z_s, z_t} + \underbrace{\left(\frac{\alpha'_s}{\alpha_s} \delta_{z_s, z_t} + \mathbf{z}_t^\top \left((\beta_s \boldsymbol{\pi}_s)' - \frac{\alpha'_s}{\alpha_s} \beta_s \boldsymbol{\pi}_s\right) \right) \Delta + o(\Delta)}_{=R_s(z_s, z_t)},\end{aligned}$$

which presents the rate matrix as claimed, concluding the proof. \square

H.4. GIDD Backward Rate

Definition H.2 (CTMC Backward Transition). For any $s < t$ with $s = t - \Delta$ and $\Delta \rightarrow 0$, we have

$$q_{s|t}(z_s|z_t) = \delta_{z_t, z_s} + \hat{R}_t(z_t, z_s) + o(\Delta),$$

where \hat{R}_t is called the backward transition rate.

Lemma H.3 (GIDD Backward Rate). *The CTMC backward rate matrix \hat{R}_t^θ of $p_\theta(z_s|z_t)$ as defined in Equation 4 is given by*

$$\hat{R}_t^\theta(z_t, z_s) = -\delta_{z_s, z_t} \sum_{z'} R_t(z', z_t) \frac{q_t(z'|x_\theta)}{q_t(z_t|x_\theta)} + R_t(z_s, z_t) \frac{q_t(z_s|x_\theta)}{q_t(z_t|x_\theta)}.$$

Proof. For the reverse rate matrix $\hat{R}_t^\theta(z_t, z_s)$, we start with our choice for the model backward transition (Eq. 4):

$$p_\theta(z_s|z_t) = q_{t|s}(z_t|z_s) \frac{q_s(z_s|x_\theta)}{q_t(z_t|x_\theta)}$$

By now setting $s = t - \Delta$ with $\Delta \rightarrow 0$, we get

$$\begin{aligned}p_\theta(z_s|z_t) &= q_{t|t-\Delta}(z_t|z_s) \frac{q_{t-\Delta}(z_s|x_\theta)}{q_t(z_t|x_\theta)} \\ &= (\delta_{z_t, z_s} + R_{t-\Delta}(z_s, z_t) \Delta + o(\Delta)) \frac{q_{t-\Delta}(z_s|x_\theta) - q'_{t-\Delta}(z_s|x_\theta) \Delta + o(\Delta)}{q_t(z_t|x_\theta)} \\ &\stackrel{\Delta \rightarrow 0}{=} \delta_{z_s, z_t} \underbrace{\frac{q_t(z_s|x_\theta)}{q_t(z_t|x_\theta)}}_{=1 \text{ if } z_s = z_t} + \underbrace{\left(\delta_{z_s, z_t} \frac{-q'_t(z_s|x_\theta)}{q_t(z_t|x_\theta)} + R_t(z_s, z_t) \frac{q_t(z_s|x_\theta)}{q_t(z_t|x_\theta)} \right) \Delta + o(\Delta)}_{=\hat{R}_t^\theta(z_t, z_s)}\end{aligned}$$

In order to get rid of the time-derivative of the forward process we use Kolmogorov's forward equation to rewrite the time-derivative of the forward process $q'_t(z_s|x_\theta)$ as $q'_t(z_s|x_\theta) = \sum_{z'} q_t(z'|x_\theta) R_t(z', z_s)$, resulting in

$$\hat{R}_t^\theta(z_t, z_s) = -\delta_{z_s, z_t} \sum_{z'} \frac{q_t(z'|x_\theta)}{q_t(z_t|x_\theta)} R_t(z', z_s) + R_t(z_s, z_t) \frac{q_t(z_s|x_\theta)}{q_t(z_t|x_\theta)}.$$

Finally, we rename z_s to z_t in the first term, since they are equal if $\delta_{z_s, z_t} = 1$ and the entire term is 0 otherwise, resulting in the desired equality:

$$\hat{R}_t^\theta(z_t, z_s) = -\delta_{z_s, z_t} \sum_{z'} R_t(z', z_t) \frac{q_t(z' | \mathbf{x}_\theta)}{q_t(z_t | \mathbf{x}_\theta)} + R_t(z_s, z_t) \frac{q_t(z_s | \mathbf{x}_\theta)}{q_t(z_t | \mathbf{x}_\theta)}.$$

□

H.5. GIDD ELBO

Our starting point is a slightly modified version of the continuous-time ELBO (CT-ELBO) from [Campbell et al. \(2022\)](#) which explicitly keeps some constant terms. Keeping these terms is useful for canceling out other terms in subsequent derivations. The proof of Proposition H.4 is largely analogous to [Campbell et al. \(2022\)](#).

Proposition H.4. *For any CTMC diffusion process with marginals $q_t(z_t | x)$, forward rate $R_t(z_s, z_t)$, and backward rate $\hat{R}_t(z_s, z_t)$, the CT-ELBO is given by*

$$\log p(x) \geq \mathbb{E}_{t, q_t(z_t | x)} \left[\hat{R}_t(z_t, z_t) - R_t(z_t, z_t) + \sum_{z_s \neq z_t} R_t(z_s, z_t) \frac{q_t(z_s | x)}{q_t(z_t | x)} \log \frac{\hat{R}_t(z_t, z_s) q_t(z_t | x)}{R_t(z_s, z_t) q_t(z_s | x)} \right] + C,$$

where $t \sim \mathcal{U}(0, 1)$ and $C = \mathbb{E}_{q_0(z_0 | x)} [\log p(x | z_0)] - D_{KL}(q_1(z_1 | x) \| p_1(x_1))$.

Proof. The key quantity in the diffusion ELBO is the KL-divergence between the true and the model backward transition, which is given by the following. For the second equality, we use Baye's rule and the fact that $q_{t|s}(z_t | z_s, x) = q_{t|s}(z_t | z_s)$ following the Markovian property of the forward process:

$$D_{KL}(q_{s|t}(z_s | z_t, x) \| p_\theta(z_s | z_t)) = \sum_{z_s} q_{s|t}(z_s | z_t, x) \log \frac{q_{s|t}(z_s | z_t, x)}{p_\theta(z_s | z_t)} \quad (10)$$

$$= \sum_{z_s} q_{t|s}(z_t | z_s) \frac{q_s(z_s | x)}{q_t(z_t | x)} \log \frac{q_{t|s}(z_t | z_s) q_s(z_s | x)}{p_\theta(z_s | z_t) q_t(z_t | x)} \quad (11)$$

In order to derive the continuous-time ELBO, we first analyze the behaviour of this term as $\Delta \rightarrow 0$ with $s = t - \Delta$. By the definition of CTMC, we then have

$$\begin{aligned} \log q_{t|s}(z_t | z_s) &= \log(\delta_{z_t, z_s} + \Delta R_s(z_s, z_t) + o(\Delta)) \\ &= \delta_{z_t, z_s} \Delta R_s(z_s, z_t) + (1 - \delta_{z_t, z_s}) \log(\Delta R_s(z_s, z_t) + o(\Delta)) + o(\Delta), \end{aligned}$$

where we use the fact that $\log(1 + x) = x - \frac{x^2}{2} + o(x^2)$ for the $z_s = z_t$ case. By also using the fact that

$$\Delta \log(\Delta x + o(\Delta)) = \Delta \log \Delta + \Delta \log(x + o(1)) = \Delta \log \Delta + \Delta \log(1 + o(1)) + \Delta \log x \xrightarrow{\Delta \rightarrow 0} \Delta \log x,$$

we then get that

$$\begin{aligned} q_{t|s}(z_t | z_s) \log q_{t|s}(z_t | z_s) &= [\delta_{z_t, z_s} + \Delta R_s(z_s, z_t) + o(\Delta)] \\ &\quad \cdot [\delta_{z_t, z_s} \Delta R_s(z_s, z_t) + (1 - \delta_{z_t, z_s}) \log(\Delta R_s(z_s, z_t) + o(\Delta)) + o(\Delta)] \\ &= \delta_{z_t, z_s} \Delta R_s(z_s, z_t) + \underbrace{\delta_{z_t, z_s} (1 - \delta_{z_t, z_s}) (\dots)}_{=0} + (1 - \delta_{z_t, z_s}) R_s(z_s, z_t) \underbrace{\Delta \log(\Delta R_s(z_s, z_t) + o(\Delta))}_{= \Delta \log R_s(z_s, z_t)} + o(\Delta) \\ &= \delta_{z_t, z_s} \Delta R_s(z_s, z_t) + (1 - \delta_{z_t, z_s}) \Delta R_s(z_s, z_t) \log R_s(z_s, z_t) + o(\Delta). \quad (12) \end{aligned}$$

By analogous reasoning, we also get that

$$q_{t|s}(z_t | z_s) \log p_\theta(z_s | z_t) = \delta_{z_t, z_s} \Delta \hat{R}_s^\theta + (1 - \delta_{z_t, z_s}) \Delta R_s(z_s, z_t) \log \hat{R}_s^\theta(z_t, z_s) + o(\Delta). \quad (13)$$

Finally, we also use the fact that

$$\begin{aligned}
 q_{t|s}(z_t|z_s) \log \underbrace{\frac{q_s(z_s|x)}{q_t(z_t|x)}}_{=0 \text{ if } z_s = z_t} &= (1 - \delta_{z_t, z_s})(\delta_{z_t, z_s} + \Delta R_s(z_s, z_t) + o(\Delta)) \log \frac{q_s(z_s|x)}{q_t(z_t|x)} \\
 &= (1 - \delta_{z_t, z_s})\Delta R_s(z_s, z_t) \log \frac{q_s(z_s|x)}{q_t(z_t|x)} + o(\Delta). \quad (14)
 \end{aligned}$$

Now we plug Equations 12, 13, and 14 into Equation 10, which yields

$$\begin{aligned}
 D_{KL}(q_{s|t}(z_s|z_t, x) \| p_\theta(z_s|z_t)) &= \\
 \Delta R_s(z_s, z_t) - \Delta \hat{R}_s^\theta(z_t, z_s) + \sum_{z_s \neq z_t} \Delta R_s(z_s, z_t) \log \frac{R_s(z_s, z_t) q_s(z_s|x)}{\hat{R}_s^\theta(z_t, z_s) q_t(z_t|x)} &= \\
 \Delta \left(R_s(z_s, z_t) - \hat{R}_s^\theta(z_t, z_s) + \sum_{z_s \neq z_t} R_s(z_s, z_t) \log \frac{R_s(z_s, z_t) q_s(z_s|x)}{\hat{R}_s^\theta(z_t, z_s) q_t(z_t|x)} \right). \quad (15)
 \end{aligned}$$

We now substitute this result into the discrete-time diffusion ELBO, which is given by

$$\begin{aligned}
 \log p(x) &\geq - \sum_{i=2}^T \mathbb{E}_{q_{\Delta i}(z_t|x)} [D_{KL}(q_{\Delta(i-1)|\Delta i}(z_s, z_t|x) \| p_\theta(z_s|z_t))] + C \\
 &= -(T-2) \mathbb{E}_{t \sim \mathcal{U}\{2\Delta, 3\Delta, \dots, (T-1)\Delta, 1\}, q_t(z_t, x)} [D_{KL}(q_{t-\Delta|t}(z_s, z_t|x) \| p_\theta(z_s|z_t))] + C,
 \end{aligned}$$

where C is the standard diffusion ELBO constant with $C = \mathbb{E}_{q_0(z_0|x)} [\log p(x|z_0)] - D_{KL}(q_1(z_1|x) \| p(x_1))$. Substituting and taking $\Delta = \frac{1}{T} \rightarrow 0$ results in the final CT-ELBO:

$$\begin{aligned}
 \log p(x) &\geq - \sum_{i=2}^T \mathbb{E}_{q_{i\Delta}(z_t|x)} [D_{KL}(q_{(i-1)\Delta|i\Delta}(z_s|z_t, x) \| p_\theta(z_s|z_t))] + C \\
 &\stackrel{s=t-\Delta}{=} - \underbrace{(1/\Delta - 2)}_{\rightarrow 1/\Delta} \mathbb{E}_{t \sim \mathcal{U}\{2\Delta, 3\Delta, \dots, (T-1)\Delta, 1\}, q_t(z_t, x)} [D_{KL}(q_{s|t}(z_s|z_t, x) \| p_\theta(z_s|z_t))] + C \\
 &\stackrel{\Delta \rightarrow 0}{=} - \frac{1}{\Delta} \mathbb{E}_{t \sim \mathcal{U}(0,1), q_t(z_t|x)} \left[\Delta \left(R_s(z_s, z_t) - \hat{R}_s^\theta(z_t, z_s) + \sum_{z_s \neq z_t} R_s(z_s, z_t) \log \frac{R_s(z_s, z_t) q_s(z_s|x)}{\hat{R}_s^\theta(z_t, z_s) q_t(z_t|x)} \right) \right] + C \\
 &= \mathbb{E}_{t \sim \mathcal{U}(0,1), q_t(z_t|x)} \left[\hat{R}_s^\theta(z_t, z_s) - R_s(z_s, z_t) + \sum_{z_s \neq z_t} R_s(z_s, z_t) \log \frac{\hat{R}_s^\theta(z_t, z_s) q_t(z_t|x)}{R_s(z_s, z_t) q_s(z_s|x)} \right] + C,
 \end{aligned}$$

which is the desired expression, concluding the proof. \square

Starting at this general form, we now plug in the forward and backward rates $R_t(z_s, z_t)$ and $\hat{R}_t(z_t, z_s)$ into Proposition H.4 and simplify the resulting expression to derive the ELBO for GIDD.

Proof of Theorem 3.7. We need to show that

$$-\log p(x) \leq \mathbb{E}_{t, z_t} [w_t(z_t, x) (D_{KL}(q_t(z_s|x) \| q_t(z_s|\mathbf{x}_\theta)) + r_\theta(z_t, x))] + \mathbb{E}_t [\alpha'_t / \alpha_t] + C,$$

with $r_\theta(z_t, x) = \frac{q_t(z_t|x)}{q_t(z_t|\mathbf{x}_\theta)} - \log \frac{q_t(z_t|x)}{q_t(z_t|\mathbf{x}_\theta)}$, $t \sim \mathcal{U}(0, 1)$, $z_t \sim q_t(\cdot|x)$, $C = \mathbb{E}_{q_0(z_0|x)} [\log p(x|z_0)] - D_{KL}(q_1(z_1|x) \| p_1(x_1))$, and the weighting function

$$w_t(z_t, x) = \frac{1}{q_t(z_t|x)} \mathbf{z}_t^\top \left((\beta_t \boldsymbol{\pi}_t)' - \frac{\alpha'_t}{\alpha_t} \beta_t \boldsymbol{\pi}_t \right).$$

We begin by noting that

$$\begin{aligned}\hat{R}_t^\theta(z_t, z_s) &= R_t(z_s, z_t) \frac{q_t(z_s | \mathbf{x}_\theta)}{q_t(z_t | \mathbf{x}_\theta)} \text{ if } z_s \neq z_t, \\ \hat{R}_t^\theta(z_s, z_t) &= - \sum_{z'} R_t(z', z_t) \frac{q_t(z' | \mathbf{x}_\theta)}{q_t(z_t | \mathbf{x}_\theta)} + R_t(z_t, z_t) \text{ if } z_s = z_t.\end{aligned}$$

Plugging this into Prop. H.4 results in

$$\log p(x) \geq \mathbb{E}_{t, z_t} \left[- \sum_{z'} R_t(z', z_t) \frac{q_t(z' | \mathbf{x}_\theta)}{q_t(z_t | \mathbf{x}_\theta)} + \sum_{z_s \neq z_t} \frac{q_t(z_s | x)}{q_t(z_t | x)} R_t(z_s, z_t) \log \frac{q_t(z_s | \mathbf{x}_\theta) q_t(z_t | x)}{q_t(z_t | \mathbf{x}_\theta) q_t(z_s | x)} \right] + C. \quad (16)$$

We now simplify the two sums inside the expectation. First, note that $R_t(z_s, z_t) = \frac{\alpha'_t}{\alpha_t} \delta_{z_s, z_t} + w_t(z_t, x) q_t(z_t | x)$. For the first sum we then get

$$\begin{aligned}\sum_{z'} R_t(z', z_t) \frac{q_t(z' | \mathbf{x}_\theta)}{q_t(z_t | \mathbf{x}_\theta)} &= \sum_{z_s} \left(\frac{\alpha'_t}{\alpha_t} \delta_{z_s, z_t} + w_t(z_t, x) q_t(z_t | x) \right) \frac{q_t(z_s | \mathbf{x}_\theta)}{q_t(z_t | \mathbf{x}_\theta)} \\ &= \sum_{z_s} w_t(z_t, x) q_t(z_s | \mathbf{x}_\theta) \frac{q_t(z_t | x)}{q_t(z_t | \mathbf{x}_\theta)} + \frac{\alpha'_t}{\alpha_t} \frac{q_t(z_t | \mathbf{x}_\theta)}{q_t(z_t | \mathbf{x}_\theta)} \\ &= w_t(z_t, x) \frac{q_t(z_t | x)}{q_t(z_t | \mathbf{x}_\theta)} + \frac{\alpha'_t}{\alpha_t}.\end{aligned}$$

For the second sum, note that $\frac{R_t(z_s, z_t)}{q_t(z_t | x)} = w_t(z_t, x)$ if $z_s \neq z_t$ and that the inner term is 0 if $z_s = z_t$ since $\log \frac{q_t(z_s | \cdot)}{q_t(z_t | \cdot)} = 0$:

$$\begin{aligned}\sum_{z_s \neq z_t} \frac{q_t(z_s | x)}{q_t(z_t | x)} R_t(z_s, z_t) \log \frac{q_t(z_s | \mathbf{x}_\theta) q_t(z_t | x)}{q_t(z_t | \mathbf{x}_\theta) q_t(z_s | x)} &= \sum_{z_s \neq z_t} w_t(z_t, x) q_t(z_s | x) \log \frac{q_t(z_s | \mathbf{x}_\theta) q_t(z_t | x)}{q_t(z_t | \mathbf{x}_\theta) q_t(z_s | x)} \\ &= w_t(z_t, x) \left(\sum_{z_s} q_t(z_s | x) \log \frac{q_t(z_s | \mathbf{x}_\theta)}{q_t(z_s | x)} + \sum_{z_s} q_t(z_s | x) \log \frac{q_t(z_t | x)}{q_t(z_t | \mathbf{x}_\theta)} \right) \\ &= w_t(z_t, x) \left(\log \frac{q_t(z_t | x)}{q_t(z_t | \mathbf{x}_\theta)} - D_{KL}(q_t(z_s | x) \| q_t(z_s | \mathbf{x}_\theta)) \right)\end{aligned}$$

Plugging both results into Eq. 16 yields

$$\begin{aligned}-\log p(x) &\leq -\mathbb{E}_{t, z_t} \left[- \left(w_t(z_t, x) \frac{q_t(z_t | x)}{q_t(z_t | \mathbf{x}_\theta)} + \frac{\alpha'_t}{\alpha_t} \right) + w_t(z_t, x) \left(\log \frac{q_t(z_t | x)}{q_t(z_t | \mathbf{x}_\theta)} - D_{KL}(q_t(z_s | x) \| q_t(z_s | \mathbf{x}_\theta)) \right) \right] + C \\ &= \mathbb{E}_{t, z_t} \left[w_t(z_t, x) \left(D_{KL}(q_t(z_s | x) \| q_t(z_s | \mathbf{x}_\theta)) + \frac{q_t(z_t | x)}{q_t(z_t | \mathbf{x}_\theta)} - \log \frac{q_t(z_t | x)}{q_t(z_t | \mathbf{x}_\theta)} \right) + \frac{\alpha'_t}{\alpha_t} \right] + C \\ &= \mathbb{E}_{t, z_t} [w_t(z_t, x) (D_{KL}(q_t(z_s | x) \| q_t(z_s | \mathbf{x}_\theta)) + r_\theta(z_t, x))] + \mathbb{E}_t [\alpha'_t / \alpha_t] + C\end{aligned}$$

with $r_\theta(z_t, x) = \frac{q_t(z_t | x)}{q_t(z_t | \mathbf{x}_\theta)} - \log \frac{q_t(z_t | x)}{q_t(z_t | \mathbf{x}_\theta)}$, thus showing the original claim and concluding the proof. \square

H.6. GIDD ELBO Global Minimum

Proof of Proposition 3.9. The global minimum of the GIDD ELBO is reached if and only if $q_t(z_t | x)$ and $q_t(z_t | \mathbf{x}_\theta)$ are the same for all x , t , and z_t . This follows from the fact that the KL-divergence is non-negative and that $D_{KL}(q_t(z_t | x) \| q_t(z_t | \mathbf{x}_\theta)) = 0$ if and only if $q_t(z_t | x) = q_t(z_t | \mathbf{x}_\theta)$ for all z . At this point, the correction term $r_\theta(z_t, x)$ also reaches its minimal value of 1, so by moving away from it can only increase the sum of both terms and hence the total ELBO. Having found a global minimum of $D_{KL}(q_t(z_t | x) \| q_t(z_t | \mathbf{x}_\theta)) + r_\theta(z_t, x) = 1$, plugging this into the GIDD

NELBO we get

$$\begin{aligned}
 -\log p(x) &\leq \mathbb{E}_{t,z_t} [w_t(z_t, x) (D_{KL}(q_t(z_s|x) \| q_t(z_s|\mathbf{x}_\theta)) + r_\theta(z_t, x))] + \mathbb{E}_t [\alpha'_t/\alpha_t] + C \\
 &= \mathbb{E}_{t,z_t} [w_t(z_t, x)] + \mathbb{E}_t [\alpha'_t/\alpha_t] + C \\
 &= \mathbb{E}_t \left[\sum_{z_t} q_t(z_t|x) \cdot \frac{1}{q_t(z_t|x)} \mathbf{z}_t^\top \left((\beta_t \boldsymbol{\pi}_t)' - \frac{\alpha'_t}{\alpha_t} \beta_t \boldsymbol{\pi}_t \right) + \frac{\alpha'_t}{\alpha_t} \right] + C \\
 &= \mathbb{E}_t \left[\mathbf{1}^\top (\beta_t \boldsymbol{\pi}_t' + \beta_t' \boldsymbol{\pi}_t) - \frac{\alpha'_t}{\alpha_t} \beta_t (\mathbf{1}^\top \boldsymbol{\pi}_t) + \frac{\alpha'_t}{\alpha_t} \right] + C \\
 &= \mathbb{E}_t \left[\beta_t \mathbf{1}^\top \boldsymbol{\pi}_t' + (1 - \alpha_t)' + \frac{\alpha'_t}{\alpha_t} (1 - \beta_t) \right] + C \\
 &= \mathbb{E}_t \left[\beta_t (\mathbf{1}^\top \boldsymbol{\pi}_t)' - \alpha'_t + \frac{\alpha'_t}{\alpha_t} \cdot \alpha_t \right] + C \\
 &= \mathbb{E}_t [\beta_t (1)'] + C \\
 &= C,
 \end{aligned}$$

showing that the global minimum the GIDD NELBO is C , thus concluding the proof. \square

H.7. Uniform Noise Ratio

Proof. We need to show that if $B = \frac{2^\gamma p_u}{N(1-p_u)}$, then the expected proportion of uniform tokens is maximal at $t = 1/2$ and equal to p_u . It is easy to see that c_t has a maximum at $t = 1/2$ and that the mass on uniform tokens is $\frac{Nc_t}{C_t}$. We then have $c_{1/2} = \frac{2^\gamma p_u}{N(1-p_u)} \cdot (1/2)^{2 \cdot \frac{\gamma}{2}} = \frac{p_u}{N(1-p_u)}$ and $\frac{Nc_{1/2}}{C_{1/2}} = \frac{Nc_{1/2}}{1+Nc_{1/2}} = \frac{\frac{p_u}{1-p_u}}{1+\frac{p_u}{1-p_u}} = p_u$, thus proving the claim. \square

H.8. GIDD ELBO Weights

We need to derive expressions for $\frac{\alpha'_t}{\alpha_t}$ and $(\beta_t \boldsymbol{\pi}_t)' - \frac{\alpha'_t}{\alpha_t} \beta_t \boldsymbol{\pi}_t$. For this, it is useful to first derive c'_t :

$$c'_t = B \left(\frac{\gamma}{2} t^{\frac{\gamma}{2}-1} (1-t)^{\frac{\gamma}{2}} - \frac{\gamma}{2} t^{\frac{\gamma}{2}} (1-t)^{\frac{\gamma}{2}-1} \right) = \frac{\gamma}{2} \left(\frac{c_t}{t} - \frac{c_t}{1-t} \right) = \frac{\gamma}{2} \frac{1-2t}{t(1-t)} c_t$$

For $\frac{\alpha'_t}{\alpha_t}$ we get

$$\frac{\alpha'_t}{\alpha} = (\log \alpha_t)' = \left(\log \frac{1-t}{C_t} \right)' = -\frac{1}{1-t} - \frac{C'_t}{C_t} = -\frac{1}{1-t} - \frac{Nc'_t}{1+Nc_t}$$

and for $(\beta_t \boldsymbol{\pi}_t)' - \frac{\alpha'_t}{\alpha_t} \beta_t \boldsymbol{\pi}_t$ we get

$$\begin{aligned}
 (\beta_t \boldsymbol{\pi}_t)' - \frac{\alpha'_t}{\alpha_t} \beta_t \boldsymbol{\pi}_t &= \alpha_t \left(\frac{\beta_t \boldsymbol{\pi}_t}{\alpha_t} \right)' = \alpha_t \left(\frac{t\mathbf{m} + c_t \mathbf{1}}{1-t} \right)' = \alpha_t \frac{(1-t)(\mathbf{m} + c'_t \mathbf{1}) + (t\mathbf{m} + c_t \mathbf{1})}{(1-t)^2} \\
 &= \frac{\mathbf{m} + (c_t + (1-t)c'_t) \mathbf{1}}{C_t(1-t)},
 \end{aligned}$$

which then is used to find $w_t(z_t, x)$:

$$\begin{aligned}
 w_t(z_t, x) &= \frac{1}{q_t(z_t|x)} \mathbf{z}_t^\top \left((\beta_t \boldsymbol{\pi}_t)' - \frac{\alpha'_t}{\alpha_t} \beta_t \boldsymbol{\pi}_t \right) = \frac{1}{q_t(z_t|x)} \mathbf{z}_t^\top \left(\frac{\mathbf{m} + (c_t + (1-t)c'_t) \mathbf{1}}{Z_t(1-t)} \right) \\
 &= \frac{\delta_{z_t, m} + c_t + (1-t)c'_t}{(1-t)(t\delta_{z_t, m} + (1-t)\delta_{z_t, x} + c_t)},
 \end{aligned}$$

In summary, the ELBO constants for our mixing schedule are given by

$$\frac{\alpha'_t}{\alpha_t} = -\frac{1}{1-t} - \frac{Nc'_t}{1+Nc_t}, \quad w_t(z_t, x) = \frac{\delta_{z_t, m} + c_t + (1-t)c'_t}{(1-t)(t\delta_{z_t, m} + (1-t)\delta_{z_t, x} + c_t)}, \quad c'_t = \frac{\gamma}{2} \frac{1-2t}{t(1-t)} c_t.$$

I. MDM as a Special Case of GIDD

We want to show that if we set $\beta_t \boldsymbol{\pi}_t = (1 - \alpha_t) \mathbf{m}$, then the GIDD ELBO recovers the MDM ELBO, i.e. it reduces to

$$-\log p(x) \leq \mathbb{E}_{t,z_t} \left[\frac{\alpha'_t}{1 - \alpha_t} \delta_{z_t,m} \mathbf{x}^\top \log \mathbf{x}_\theta(Z_t, t) \right] + C.$$

To show this, we first take a look at how individual terms of the GIDD ELBO simplify for this choice of $\beta_t \boldsymbol{\pi}_t$. First, note that $(\beta_t \boldsymbol{\pi}_t)' = -\alpha'_t \mathbf{m}$ and hence

$$w_t(z_t, x) = \frac{1}{q_t(z_t|x)} \mathbf{z}_t^\top \left(-\alpha'_t \mathbf{m} - \frac{\alpha'_t}{\alpha_t} (1 - \alpha_t) \mathbf{m} \right) = \frac{1}{q_t(z_t|x)} \delta_{z_t,m} \left(\frac{-\alpha'_t(1 - \alpha_t) - \alpha'_t \alpha_t}{\alpha_t} \right) = -\frac{1}{q_t(z_t|x)} \frac{\alpha'_t}{\alpha_t} \delta_{z_t,m}.$$

We can see that the weight of any non-mask token is 0, so we can focus on simplifying the term inside the expectation of the GIDD ELBO assuming that $z_t = m$. In that case, we have $q_t(m|x) = q_t(m|\mathbf{x}_\theta) = (1 - \alpha_t)$, $q_t(x|x) = \alpha_t$, $q_t(z_t \notin \{x, m\}|x) = 0$, $q_t(z_t \neq m|\mathbf{x}_\theta) = \alpha_t \mathbf{z}_t^\top \mathbf{x}_\theta(Z_t, t)$, and therefore

$$\begin{aligned} D_{KL}(q_t(z_s|x) \| q_t(z_s|\mathbf{x}_\theta)) + r_\theta(z_t, x) &= \sum_{z_s} q_t(z_s|x) \underbrace{\log \frac{q_t(z_s|x)}{q_t(z_s|\mathbf{x}_\theta)}}_{=0 \text{ if } z_s = m} + \underbrace{\frac{q_t(m|x)}{q_t(m|\mathbf{x}_\theta)}}_{=1} - \underbrace{\log \frac{q_t(m|x)}{q_t(m|\mathbf{x}_\theta)}}_{=0} \\ &= \sum_{z_s \neq m} q_t(z_s|x) \log \frac{q_t(z_s|x)}{q_t(z_s|\mathbf{x}_\theta)} + 1 \\ &= q_t(x|x) \log \frac{q_t(x|x)}{q_t(x|\mathbf{x}_\theta)} + 1 \\ &= -\alpha_t \log(\alpha_t \mathbf{x}^\top \mathbf{x}_\theta(Z_t, t)) + \alpha_t \log \alpha_t + 1 \\ &= -\alpha_t \mathbf{x}^\top \log \mathbf{x}_\theta(Z_t, t) + 1. \end{aligned}$$

Combining the two results then yields

$$\begin{aligned} -\log p(x) &\leq \mathbb{E}_{t,z_t} [w_t(z_t, x) (D_{KL}(q_t(z_s|x) \| q_t(z_s|\mathbf{x}_\theta)) + r_\theta(z_t, x))] + \mathbb{E}_t [\alpha'_t / \alpha_t] + C \\ &= \mathbb{E}_{t,z_t} \left[-\frac{1}{q_t(z_t|x)} \frac{\alpha'_t}{\alpha_t} \delta_{z_t,m} (-\alpha_t \mathbf{x}^\top \log \mathbf{x}_\theta(Z_t, t) + 1) \right] + \mathbb{E}_t \left[\frac{\alpha'_t}{\alpha_t} \right] + C \\ &= \mathbb{E}_{t,z_t} \left[\frac{\alpha'_t}{1 - \alpha_t} \delta_{z_t,m} \mathbf{x}^\top \log \mathbf{x}_\theta(Z_t, t) - \frac{\alpha'_t}{\alpha_t} \frac{1}{1 - \alpha_t} \delta_{z_t,m} \right] + \mathbb{E}_t \left[\frac{\alpha'_t}{\alpha_t} \right] + C \\ &= \mathbb{E}_{t,z_t} \left[\frac{\alpha'_t}{1 - \alpha_t} \delta_{z_t,m} \mathbf{x}^\top \log \mathbf{x}_\theta(Z_t, t) \right] - \underbrace{\mathbb{E}_t \left[q_t(z_t = m|x) \frac{\alpha'_t}{\alpha_t} \frac{1}{1 - \alpha_t} - \frac{\alpha'_t}{\alpha_t} \right]}_{=0} + C \\ &= \mathbb{E}_{t,z_t} \left[\frac{\alpha'_t}{1 - \alpha_t} \delta_{z_t,m} \mathbf{x}^\top \log \mathbf{x}_\theta(Z_t, t) \right] + C, \end{aligned}$$

which shows that GIDD is equivalent to MDM if $\beta_t \boldsymbol{\pi}_t = (1 - \alpha_t) \mathbf{m}$.

J. Unconditional Generation

Here we provide examples from our mask-only and our mask + uniform ($p_u = 0.2$) model, with each sample presented twice: Once before self-correction and after the self-correction step applied with a temperature $\tau = 0.1$.

J.1. GIDD+ BASE, $p_u = 0.0$

This is our mask-only model which achieves best results on language understanding benchmarks. Due to being trained without uniform noise, sample quality is not improved by the self-correction step, neither qualitatively nor quantitatively.

J.1.1. EXAMPLE 1

No self-correction.

There's always something to please media fans, but this time you've got the vitriolic backlash to Hollywood mistakes on 20th Century Fox, including the foolish idea to remind people of the history of the Star Wars movies, first seen as sci-fi. And the story is UK-based, News. Daily, as if noting the video-based example of journalism have a news filing need to suggest the fine-instrument: Bad News. Sadly, the resulting outrage here is no longer the -big-rdrob but more-actual. News in the world, the front pages touting the studios' contribution are something you could read without caution: "4 million people at Fox re-find in the past month to have exposed bodies." Not anytime anyone Fox movies I see this storyline on the Fox channel, but increasingly it's just been said all around you. Light sidelines miss James Cameron in 2003, for re-creating the original Terminator franchise to such acclaim. News that his films now seems to have more outraged those who regularly spend money/trying to watch the original Tv shows. Long before the current 'settling' between their two studios that the artifact lasts and prevailed, it is became easy, and people entertained, for a program chosen by taste to be hit. And the end results proved close to these three. *For the new day use "fairly"" that sentence...

Update:

h/t DruurlifeTriviaInBoston, and MightyJamesJade: ON,

Watch the proud-anti-Star Wars skit from Hollywood

Self-corrected ($\tau = 0.1$)

There's always something to please media fans but this time you've got the vitriolic backlash to Hollywood mistakes on 20th Century Fox,

very idea to remind people of

of the A Wars movies, first seen as sci-fi. And the story is UK-based, News. Daily, as if noting the video-based example of journalism have a news filing need to suggest the fine-instrument: Bad News. Sadly, the resulting outrage here is no longer the -big-rdrob but more-actual. News in world, the front pages touting the studios' contribution are something you could read without caution: "4 million people at Fox re-find in the past month to have exposed bodies." Not anytime anyone Fox movies I see this storyline on the Fox channel, but increasingly it's just been said all around you. Light sidelines miss James Cameron in 2003, for re-creating the original Terminator franchise to such acclaim. News that his films now seems to have more outraged those who regularly spend money/trying to watch the original Tv shows. Long before the current 'settling' between their two studios that the artifact lasts and prevailed, it is became easy, and people entertained, for a program chosen by taste to be hit. And the end results proved close to these three. *For the new day use "fairly"" that sentence...

Update:

h/t DruurlifeTriviaInBoston, and MightyJamesJade: ON,

Watch the proud-anti-Star Wars skit from Hollywood

J.1.2. EXAMPLE 2

No self-correction.

[...] confiscation of their weapons from neighbors and supplies, and expropriation become the organizational sectors of assembly, production, and production. Roadblocks became increasingly difficult until the emergence of

Hellfire missiles from the US. Production is more difficult due to logistical organizations provided by the US using the M4682/Chad drop pup (Csharp") 1864 rifles.

There are several other groups working in the area but are well known there: the village fighters can collectively run a country, both in terms of fighting power and in the supply of materials (669 show and other chief wrapped clothing, and inoys supply 86 bolts) without the huge movement needed to expand through the Africa.

The groups who operate in Libya are also logistics-driven. They have a fantastic operational networks organizing members to retap their raids; the group is how to control strategic kerbs, the constant addition of the group often taking approach of a legal generating street marketing place, where the shop shuts up forcing the vendors to relocate out of the area. It is also possible to observe the ability to locate and approach frequently at checkpoints.

Fakesters are an area of danger assent. Members capture all office holders, deputies, officials, and candidates fleeing to Tripoli have to pass through our protected areas, so there are lots of opportunity to stop the leader protests taking place outside such locations and and it is gone they simply perform minor scenes elsewhere in the protected area overnight. The group was able to organize to move refugees into an attacking militia stronghold in Eastern Liby, at a morally sensitive site. Plenty of people were kidnapped only days later. This gives the very large number of heavy armored vehicles in - weapons gain access means by using the gravel mines abandoned there many years ago. These vehicles are also concerned with internal security, for Libya has no Province, or no power, but to have ethnicity, even a despot.

Later in 2003, the group took control of the incarceration of Kostaeil, the commercial capital of Apeda, where the large produoil but by perc export value additional background groups have increased intervention and intrigue into the business sector and on the intelligence scene:

One invention is in the informal community of Umesu Bil where a background group, armed to well established cells, infiltrated some insurgent installations in advance through the town of Kostaeil. The abduction targets individuals with intelligence (punding of local language), one especially, Mr. Halroy from the U.S noted what was happening and who noted that Mrs. [...]

Self-corrected ($\tau = 0.1$).

[...] dation of their weapons from the and supplies, and exp the, become the organizational sectors of assembly, production, and production. Roadblocks became increasingly difficult with the emergence of Hellfire missiles from the US. The is more difficult due to the group provided by the US using the M4682/Ch, drop pup (plsharp) and the rifles.

The are several other groups working in the area but are well- there: the village fighters to the run the country, both in terms of fighting, and in the supply of, the669 show, the chief wrapped clothing, and in the supply of, the without the huge movement needed to expand through the Africa.

The groups who operate in Libya are also logistics-driven. They have a high operational networks organizing members to retap their raids, the group is how to control the kerbs, the constant addition of the group often taking approach of a legal generating street marketing place, where the shop shuts up forcing the vendors to relocate out of the area. It is also possible to observe the ability

to locate and approach frequently at the.

The group are an area of danger assent. They capture the office holders, deputies, officials, and candidates fleeing to, have to pass though the back areas, so they are a of opportunity to stop the leader protests taking place outside the locations and and in is gone, to perform minor scenes elsewhere in the protected area overnight. The group was the to organize to the refugees into the the militia stronghold in Eastern Libia, at a morally sensitive site. Plenty of people were kidnapped only days later. The group has a fair number of heavy armored vehicles in the to gain the means by the the gravel mines abandoned in many years ago. The group are also the with internal security, for Libya has no Province, and no government, but to have ethnicity, and a despot.

The in 2003, the group took control of the town of Kostaeil, the commercial capital of the country, where the large produ, but by perc export value additional background groups have increased the and intrigue in the business sector and on the intelligence scene.

One invention is in the informal community of Umesu, where a background group, armed to well in cells, infiltrated some the installations in the through the town of Kostaeil. The abduction targets individuals with intelligence (punding of local language), one especially, Mr. Halroy from the U.S noted what was happening and who noted that Mrs. [...]

J.2. GIDD+ BASE, $p_u = 0.2$

This is our best model trained on a combination of masking and uniform noise. It achieves the best sample quality as measured by generative PPL. Thanks to being trained on some amount of uniform noise, it is able to identify and correct mistakes, which allows it to improve sample quality during the self-correction step, both qualitatively and quantitatively.

J.2.1. EXAMPLE 3

No self-correction.

NBC Community Mystery Science Tour: let's talk about it. Though the Abrams's show is about to drop cable this October, the second season looks squarely at NBC, which confirms what a deal the network is in to as the family comedy follows CBS Studios for its third (sp) season. With that said, I have another (unjustified) update: Season 2 is in.

You know how ABC is breaking up on the word "GOSH" to "BLOOD MIDNLE AND COOLORN" they share Calm similarities with? This #Indybookforecnt1 meme should make it familiar in your head pic twitter.com/ZvonWolfsp/7F6SF-H -- Agent Cole (@AgentBlow) July 2, 2016

Ayes of Tumblr and AnchorGateHQ have had fun putting together this pic of Alison Brie/Bobby Bure wandering down a Twin Peaks street. Is that his family's recent death? Kid Cumberbatch dedication to DH (or Mount) is a direct nod to Twin Peaks' creator David Lynch?

There's nothing good from this pic: It used to be similar. Teddy Tu's wearing the same scarf for a while. Charlie and son Paradise are all connected.

Cumberbatch is having some Scullyian fun here, and it's followed later by another "Thanks John, is it?"

Jess Bure and Benedict had it as a heinous serial killer, but then Forest Whitaker and his neighbor did the same thing.

ABC still also won't confirm that Tony Hale will return given a role for Season 3

(or that he will be coming back as co-star on the show).

What do we think? Will CBS watch Community again next year, America? Yunande Mask

Self-corrected ($\tau = 0.1$).

The Community Mystery Science Series, let's talk about it. Though the show's show is about to hit it in October, the first season is focused on Community, which confirms what a place the show is in, as the family comedy leaves CBS Television after its third (second) season. With that said, we have a (via Classified) update: Season 2 is in.

You know how Community is breaking up from the word "JOSH" to "BLACKSTYLE AND COLLORN" they share a name with? This #Indybookforecnt1 pic will make that stick in your head. <https://twitter.com/ZvonWolfsp/7F6SF-H> | Agent Blow (@AgentBlow) July 2, 2016

Eyes of Community and Anchor News Network have had fun putting together this pic of Alison Brie/Brie Brie wandering down a Twin Peaks street. Is it the show's recent death, Benedict Cumberbatch returning to Community (or Mount) or a direct reference to Twin Peaks' creator David Lynch?

There's nothing good in this pic. Community used to be dead. Community has been wearing the same scarf for a while. Community and Twin Peaks are not connected.

Cumberbatch is having some Lynchian fun here, and it's followed up by a "Thanks John, is it?"

Jess Brie and Benedict had fun as a heinous serial killer, but then Forest Whitaker and his neighbor did the same thing.

Community has also won't confirm whether Tony Hale will be playing a role in Season 3 (or whether he will be coming back as co-star on the show).

What do you think? Will you watch Community again next year, America?

J.2.2. EXAMPLE 4

No self-correction.

[...] oil;) Tul serious bid here for OPEC news to be operational for U-T policy. The most interesting part is that it there, "Ask Exxon, out of it" in an internal investigation though secret that formerly also bankrolls the oil companies is equally interesting. Even though the biggest drubble been Petro-Exxon Corporation, there is four bidding to third international pads. Price is in fact the greying glare in that original story. One of these, being overseen by Mr. Slovakia, has a mystery poker to any one, and to officials in the kingdom. He always finds that the price of oil and gas rises (yes 'other) therefore a relief will come to go buy the giants of oil reserves at maturity. Then the boom will begin. See, the government has gone on their way.

At the outset, Exxon he was a major corporate investment. At the longest point of time Mr. Redi was all generous of support for others, and and importantly of all he has a wife, USPOC expembaddin SaathJu who is a very Low colored Oil Minister with a funny eye. But on that grand reform she went off the shelf to his bandwagon.

The raj, these are all phases, have had little impetus encouraged, as with the Saudi reversal. Yet the business has been on ice as confusion, as the be discovered small moment left with students of production and 2010, will be tasked

with determining what to do now.

In a struggle over the link in oil of gas sales, they would be including exports, Gulf States for LPG, Iraqi government oil for export and even encouraged EN leaders are emboldening the time of knocking down theigsaw to the funnatively new renaissance that Iraq appears to have,^{1[?]} which will be going to China, without counting oil. China will likely invest in crude, and then on top of the country imports, along with shale gas to meet current needs. They have been most approved of the fact that a more stable pipeline between refinery refineries means there prosperity "live the clean room," quant crude does, and cover the hole.

While the idea of PetroWestman was ignited, by All Sugar Taylor, of the Chaotic Oil when it was conceived to work so far, Exchange and oil businessmen have been less eager to see in this spirit as oil production has been far slower than anybody imagined. With the factors cause been oil prices of the 80s declining, and the surging price of heavy countermarket oil and gas [...]

Self-corrected ($\tau = 0.1$).

[...] oil; and a new bid, to OPEC, to be operational the U-T policy. The most interesting part is that the there,-Saudi, is out of it, and the internal, Exxon, which formerly also bankrolls the oil, is not interesting. Even though the new drabble is Saudi-Exxon Corporation, there are four bids to the international cartel. This is in fact the tidying part of the original plan. One of these, being overseen by Mr. Slovakia, is a mystery, to the one, and to officials in the kingdom. He always finds that the price of oil and gas rises (the-other) and the time will come to go buy the giants of the oil in Iraq. Then the boom will begin. See, the government has gone on the way.

At the time, Exxon he was a major corporate investment. At the same point of time Mr. Redi was all generous of support to others, and most important of all he has a wife, USPOC-embaddin Saath, who is a very Low, and Minister with a funny eye. But on the grand reform she is on the way to the bandwagon.

The raj, which are the phases, have been little impetus encouraged, as with the Saudi reversal. Yet the business has been on ice as well, as the newly discovered oil moment, with students of production in 2010, will be tasked with deciding what to do next.

In the struggle of the link of oil and gas sales, which will be including exports to Gulf States for LNG and Iraqi government oil for export, even the EN leaders are emboldening the idea of knocking out theigsaw of the funnatively new oil that Iraq appears to have, which will be sold to China, without the oil. They will likely buy the oil, and then on top of the country oil, along with shale gas to meet their needs. They have been most approved of the fact that a more stable pipeline to the refineries means more oil, in the clean room, as crude does, and in the hole.

While the idea of Petro-Iraq was ignited, by the Sugarman, and the Chaotic, when it was conceived to work so far, Exchange and oil businessmen have been less eager to participate in it, as oil production has been much slower than they expected. With the main price of oil, in the 80s declining, and the surging price of the upmarket oil and gas [...]